Design and Development of a Portable Bio-impedance Based Device for Foot Analysis

Shreenandan Sahu

Department of Applied Mechanics and Biomedical Engineering

Indian Institute of Technology Madras

Design and Development of a Portable Bio-impedance Based Device for Foot Analysis

Dissertation submitted in partial fulfilment of the Requirement for the degree of

Master of Technology

In

Clinical Engineering

By

Shreenandan Sahu

(Roll NO: ***CL24M013)***

Under the guidance of

Prof. Boby George

May 2026

Department of Applied Mechanics and Biomedical Engineering

Indian Institute of Technology Madras

Declaration of Originality

I, Shreenandan Sahu, Roll Number CL24M013, hereby declare that this dissertation entitled "**Design and Development of a Portable Bio-impedance Based Device for Diabetic Foot Analysis**" represents my original work carried out at the Indian Institute of Technology Madras in partial fulfilment of the requirements for the degree of Master of Technology in Clinical Engineering. To the best of my knowledge, this dissertation contains no material previously published or written by another person, nor any material submitted for the award of any degree or diploma of this or any other institution.

Any contributions made to this research by others, with whom I have collaborated at IIT Madras or elsewhere, have been appropriately acknowledged in this dissertation. All sources of information and references used in this work have been duly cited under the appropriate sections of the dissertation.

I further declare that the work presented in this dissertation has been carried out under the guidance of Prof. Boby George, Department of Electrical Engineering, IIT Madras, and that all experimental results, analyses, and interpretations presented are based on my original work unless otherwise stated.

I understand that in the event of any discrepancy or violation of academic integrity detected in the future, the Institute reserves the right to take appropriate action in accordance with its academic regulations.

May 08, 2026

IIT Madras

Shreenandan Sahu

Acknowledgement

I would like to express my sincere gratitude to my supervisor, Prof. Boby George, Department of Electrical Engineering, Indian Institute of Technology Madras (IIT Madras), for his constant guidance, valuable suggestions, encouragement, and support throughout the course of this project. His insights and mentorship greatly helped in shaping the direction and successful completion of this work.

I would also like to thank all the faculty members and staff who provided the necessary resources and support during the development of this project.

I extend my heartfelt gratitude to my lab mates, friends, and colleagues for their continuous encouragement, discussions, and support throughout the project. Their assistance and motivation made the entire development process both productive and enjoyable.

Finally, I would like to express my deepest gratitude to my parents and family for their unwavering support, patience, and encouragement at every stage of my academic journey. Their trust and motivation have always been a major source of strength and inspiration.

May 8, 2026

IIT Madras

Shreenandan Sahu

CL24M013

Abstract

This work presents the design and development of a portable multi-point bio impedance measurement system for localized foot impedance analysis using frequency sweep-based tissue characterization. The proposed system integrates an AD5934 impedance measurement unit, analog front-end circuitry, electrode multiplexing, calibration circuitry, and an ESP32-WROOM-32 microcontroller into a compact custom-designed PCB platform. A dedicated 3D-printed foot interface incorporating PCB-based electrodes was developed to enable repeatable impedance acquisition from multiple predefined foot regions. The embedded firmware controls electrode selection, calibration, and frequency sweep operations, while a Python-based software interface enables real-time data acquisition, processing, visualization, and storage.

Preliminary impedance measurements were performed over a frequency range of 1 kHz to 100 kHz to evaluate the frequency-dependent electrical behavior of biological tissue. Experimental measurements conducted across multiple body regions including the heel, ankle, elbow, and thumb demonstrated clear and repeatable impedance trends. The measured impedance decreased with increasing frequency across all regions, consistent with the expected capacitive behavior of biological tissues. Distinct impedance variations were also observed between different tissue types and skin conditions, with regions such as the ankle and elbow exhibiting comparatively higher impedance values than softer and more hydrated regions. Although full multi-point calibration is still under development, the obtained trends validate the functionality and feasibility of the proposed portable bio impedance measurement system.

Keyword: *Foot Impedance Analysis, AD5934, ESP32, Frequency Sweep, Tissue Characterization, Diabetic Foot, Embedded System, Multi-point Measurement.*

List of Contents

List of Figures

"Dedicated to the Almighty, my Supervisor Prof Boby George, my parents and my lab mates"

Chapter 1: Introduction

1.1.Introduction to Diabetic Foot and Bio impedance Analysis

Diabetes mellitus is a chronic metabolic disorder characterized by elevated blood glucose levels resulting from insufficient insulin production, impaired insulin action, or both. Prolonged hyperglycemia can lead to several microvascular and macro vascular complications, including neuropathy, peripheral vascular disease, and impaired wound healing. Among these complications, diabetic foot conditions represent a major clinical concern due to their association with tissue degeneration, ulcer formation, infection, and possible amputation. Early identification of tissue-level changes in the foot is therefore essential for preventive monitoring and timely clinical intervention.

Bioimpedance analysis has emerged as a promising non-invasive technique for studying the electrical properties of biological tissues. Biological tissues exhibit both resistive and capacitive behavior due to the presence of extracellular fluids, intracellular fluids, and cell membranes. By applying a small alternating current signal over a range of frequencies and measuring the corresponding electrical response, impedance characteristics of tissue can be obtained. Since tissue structure, hydration, vascularity, and cellular integrity influence electrical impedance, bioimpedance measurements can potentially provide useful information regarding physiological and pathological tissue conditions.

In diabetic foot conditions, ischemia, neuropathy, tissue degradation, and reduced perfusion can alter the electrical properties of the affected tissue. Such structural and physiological changes may result in measurable variations in tissue impedance. Additionally, different regions of the foot experience varying pressure distributions and tissue stresses, leading to localized differences in impedance characteristics. This highlights the importance of multi-point impedance acquisition rather than single-point measurement approaches.

The present work focuses on the development of a portable multi-point bioimpedance measurement system for localized foot tissue analysis. The system utilizes an AD5934-based impedance measurement frontend integrated with an ESP32-WROOM-32 microcontroller, electrode multiplexing circuitry, calibration networks, and a Python-based software interface for data acquisition and visualization. The proposed device aims to provide a compact and configurable platform for frequency-dependent impedance characterization of foot tissue, while enabling future studies involving tissue condition assessment and diabetic foot analysis.

1.2. AIM and OBJECTIVES

Aim

To design and develop a portable multi-point bio impedance measurement system for frequency-dependent foot tissue analysis.

Objectives

- Design and develop a portable embedded bio impedance measurement system using AD5934 and ESP32-WROOM-32.
- Develop a multi-point electrode interface and foot platform for localized impedance acquisition from different regions of the foot.
- Implement frequency sweep-based impedance measurement and calibration techniques for tissue characterization.
- Develop embedded firmware and a Python-based software interface for real-time data acquisition, visualization, and storage.
- Evaluate impedance variations across different tissue and skin conditions through experimental measurements.
- Analyze frequency-dependent impedance trends and spatial variations across multiple body regions and foot locations.
- Investigate the feasibility of using localized bio impedance measurements for future diabetic foot-related studies.

Chapter 2: Literature Review

2.1. Blood Glucose Homeostasis

Blood glucose homeostasis refers to the regulation of blood glucose levels within a narrow physiological range despite variations in dietary intake and metabolic demand. Following the ingestion of carbohydrates, glucose is produced during digestion and absorbed into the bloodstream through the small intestine, leading to an increase in blood glucose concentration. The pancreas continuously monitors these levels and responds by releasing insulin from beta cells during elevated glucose conditions and glucagon from alpha cells when glucose levels decline. These hormones work in coordination to maintain glucose balance. [1]

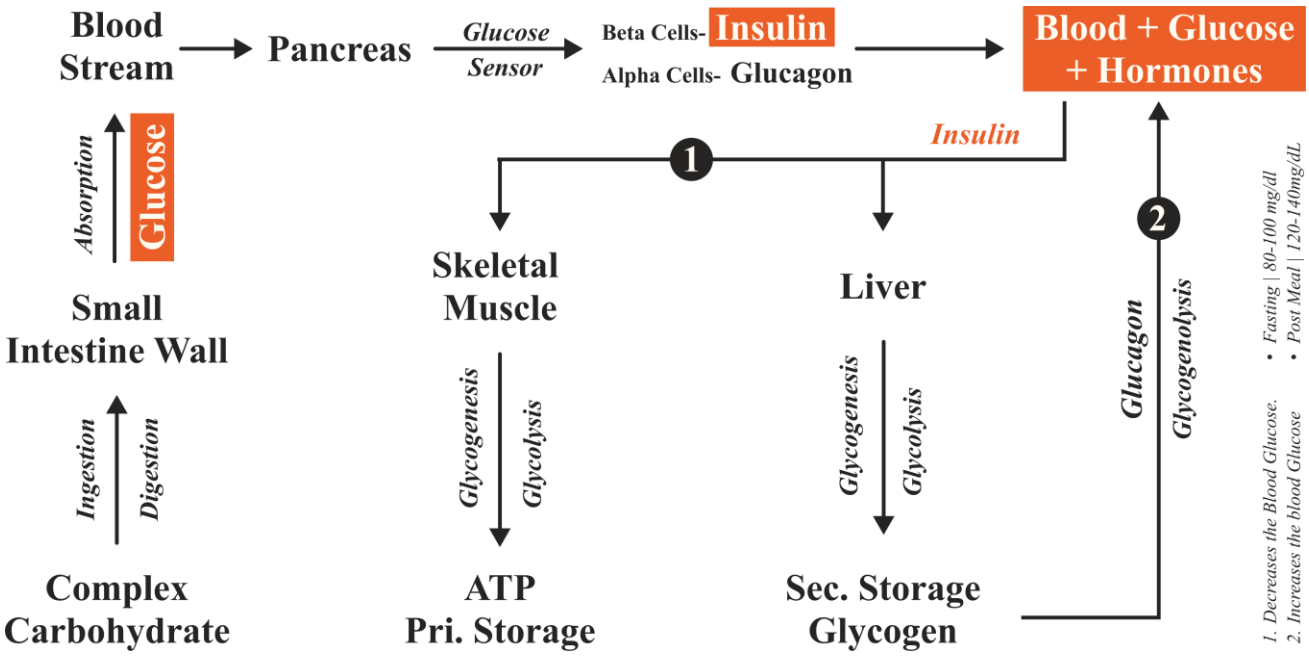

Figure 1:- Schematic representation of blood glucose homeostasis illustrating the roles of insulin and glucagon in regulating glucose uptake, storage, and release across major organs.

Insulin primarily acts during elevated blood glucose levels, such as in the postprandial state. It facilitates the uptake of glucose into tissues, particularly skeletal muscle, where it is utilized for energy production in the form of ATP. Additionally, insulin promotes glycogenesis, enabling excess glucose to be stored as glycogen in muscle and liver tissues. The liver functions as a key storage organ, helping regulate excess glucose and maintain systemic balance. [1]

In contrast, during periods of low blood glucose, such as fasting, glucagon is released to restore normal levels. It stimulates glycogenolysis in the liver, leading to the release of glucose into the bloodstream, and also promotes gluconeogenesis. This ensures a continuous supply of glucose to vital organs, particularly the brain. The coordinated action of insulin and glucagon maintains blood glucose levels within a stable physiological range.[1]

2.2. Hyperglycemia and its Causes:

Hyperglycemia or elevated blood glucose levels, is a defining feature of diabetes mellitus and arises when the body is unable to properly regulate glucose. Under normal conditions, insulin produced by the pancreatic beta cells enables glucose uptake into tissues and maintains metabolic balance. However, factors such as lifestyle, environmental influences, genetic predisposition, and aging can disrupt this regulation. As a result, either insulin production becomes insufficient or the body's response to insulin is impaired, leading to sustained high blood glucose levels.

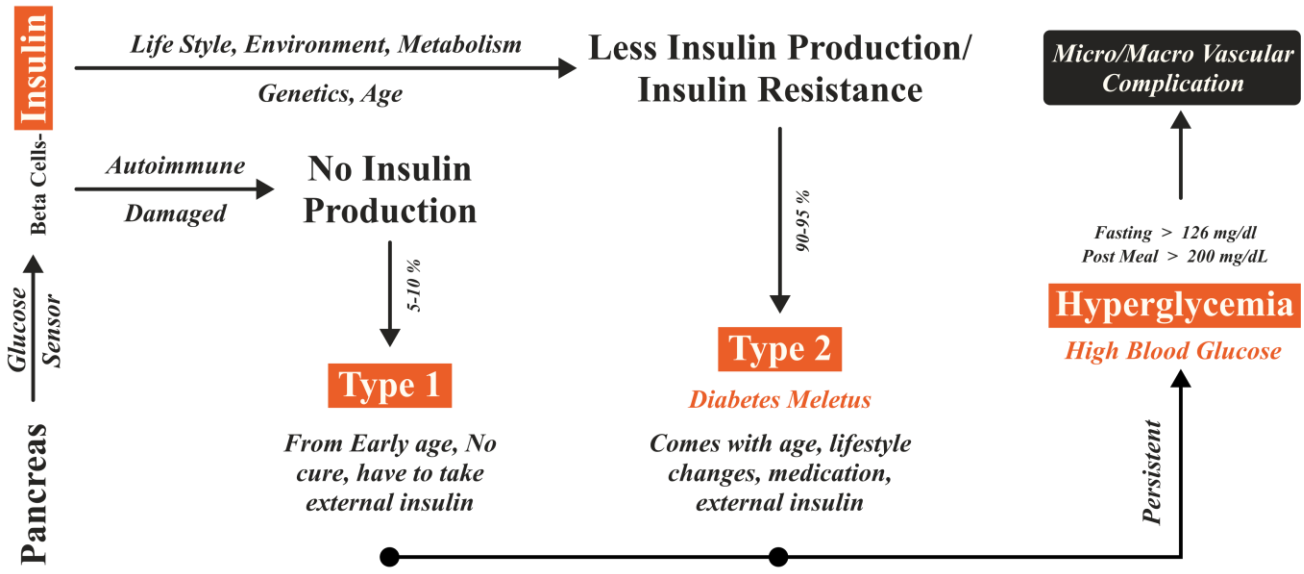

Figure 2:- Overview of hyperglycemia and diabetes showing the roles of insulin deficiency and insulin resistance, along with progression to complications.

Diabetes is broadly classified into two main types based on the underlying mechanism. Type 1 diabetes results from autoimmune damage to the pancreatic beta cells, leading to little or no insulin production. It is typically observed at an earlier age and requires lifelong external insulin administration. In contrast, Type 2 diabetes is far more common and is primarily associated with

insulin resistance, where the body does not effectively respond to insulin despite its presence. This condition is often influenced by lifestyle factors such as diet, physical inactivity, and obesity, and may require a combination of lifestyle modification, medication, and sometimes insulin therapy for management.

Persistent hyperglycemia over time can lead to serious complications affecting both small and large blood vessels. These include microvascular complications such as neuropathy, retinopathy, and nephropathy, as well as macro vascular conditions like cardiovascular disease. Clinically, hyperglycemia is identified when fasting blood glucose exceeds approximately 126 mg/dL or postprandial levels rise above 200 mg/dL. Continuous exposure to elevated glucose levels contributes to progressive tissue damage, highlighting the importance of early monitoring and effective management.

2.3. Complications due to Hyperglycemia:

Chronic hyperglycemia, when not adequately managed, gradually affects the vascular system and leads to a wide range of complications. These complications are broadly categorized into macrovascular and microvascular disorders based on the size of the blood vessels involved. Macrovascular complications affect larger arteries and are associated with conditions such as coronary heart disease and cerebrovascular disease, increasing the risk of heart attacks and strokes. On the other hand, microvascular complications involve smaller vessels, leading to conditions like diabetic retinopathy and nephropathy, which affect the eyes and kidneys respectively.

A particularly important macrovascular complication in the context of the lower limbs is peripheral vascular disease. This condition is characterized by reduced blood flow due to atherosclerosis, where arterial walls thicken and narrow. Over time, this reduced circulation can lead to tissue damage, resulting in ulceration, delayed wound healing, and in severe cases, gangrene. The lack of adequate blood supply, also referred to as ischemia, plays a critical role in the progression of these conditions, especially in the feet where circulation is already more vulnerable.

In addition to vascular issues, diabetic neuropathy significantly contributes to foot-related complications. This includes peripheral (sensory), autonomic, and motor neuropathy, each affecting nerve function in different ways. Sensory neuropathy reduces the ability to feel pain or injury, while motor neuropathy can lead to deformities that increase pressure points on the foot. Autonomic neuropathy affects sweat and oil gland function, leading to dry and cracked skin, which increases the

risk of infection. The combined effect of poor blood supply and nerve damage forms the primary underlying cause of diabetic foot disease, making early monitoring and assessment essential.

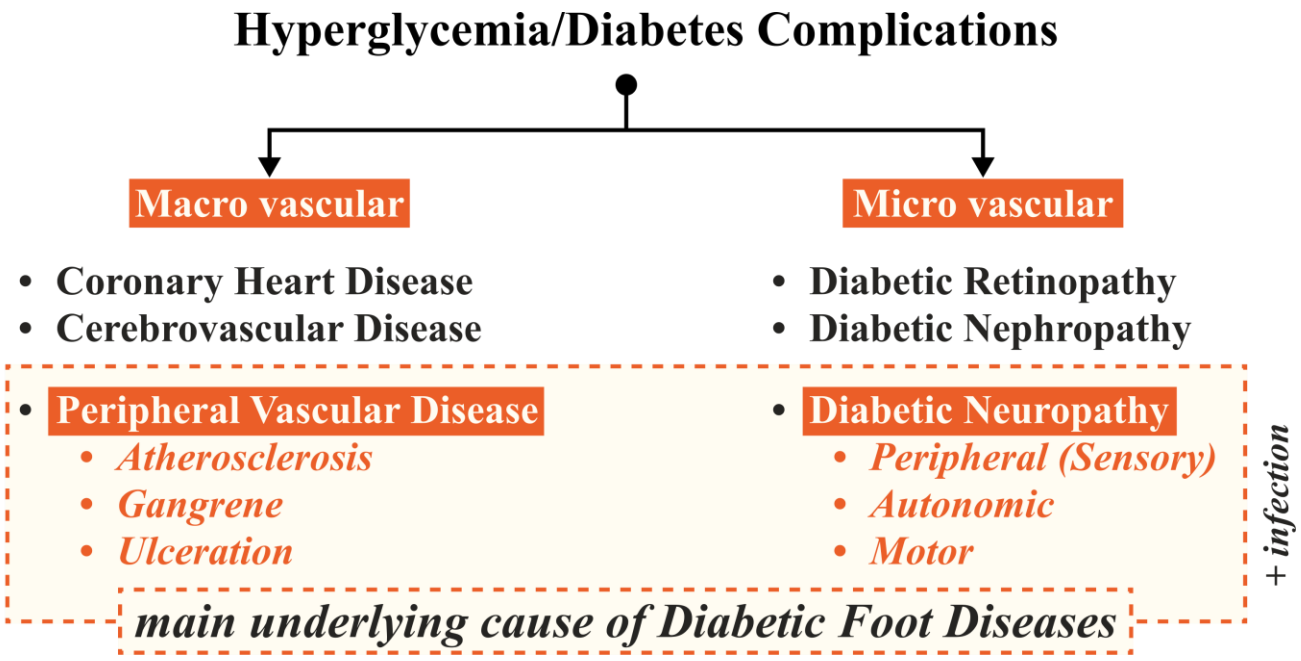

Figure 3:- Overview of macro vascular and microvascular complications of hyperglycemia, highlighting their role in the development of diabetic foot conditions.

2.4. Pathophysiology of Vascular Changes in Hyperglycemia:

The process begins with persistently elevated blood glucose levels, where excess glucose enters endothelial cells lining the blood vessels even without insulin regulation. Inside these cells, glucose undergoes metabolic pathways that generate reactive byproducts such as reactive oxygen species (ROS), advanced glycation end products (AGEs), and activation of protein kinase C (PKC). These biochemical changes create a state of cellular stress and damage, impairing normal endothelial function. As a result, the vascular lining becomes more permeable and prone to dysfunction.

This increased permeability allows low-density lipoproteins (LDL) and circulating monocytes to penetrate the vessel wall. Monocytes differentiate into macrophages, which engulf LDL particles and transform into foam cells. The accumulation of these foam cells marks the early stage of atherosclerotic plaque development. Alongside this, inflammatory signaling intensifies, releasing cytokines that further damage the vessel wall. Smooth muscle cells (SMCs) from the tunica media begin to proliferate and migrate toward the inner layers, contributing to structural changes in the vessel.

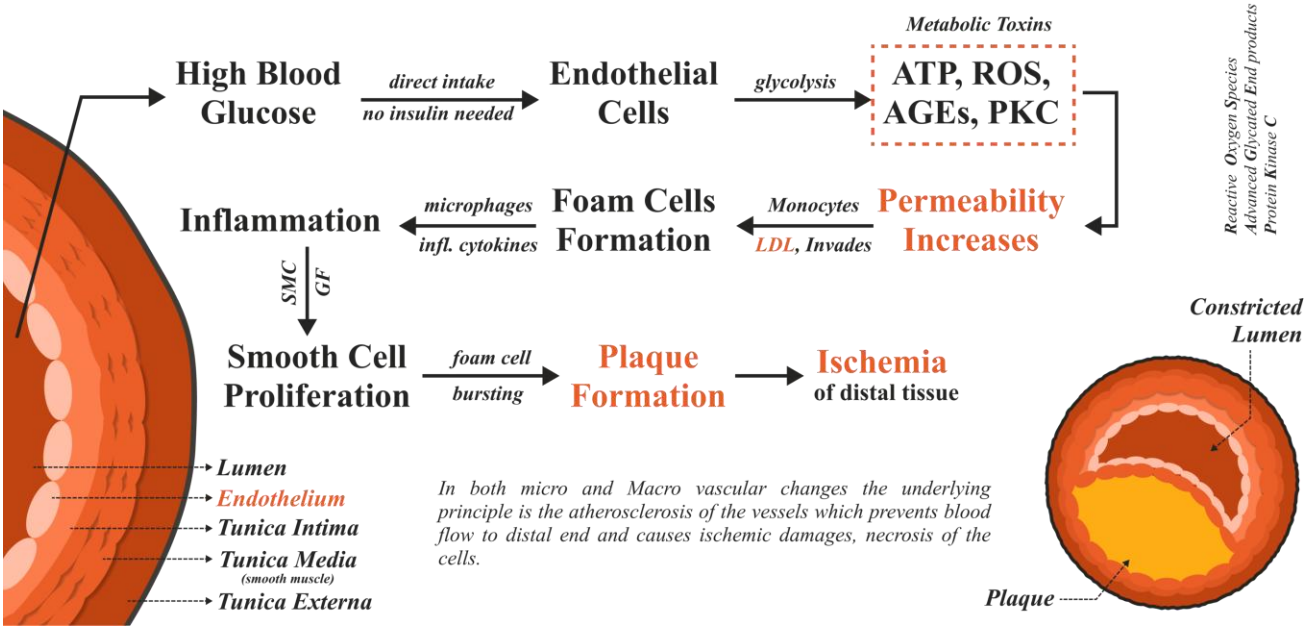

Figure 4:- Sequence of endothelial dysfunction and atherosclerotic plaque formation leading to reduced blood flow and ischemia under chronic hyperglycemia.

As the process progresses, foam cells may rupture, and lipid accumulation continues, leading to the formation of a mature plaque within the arterial wall. This plaque gradually narrows the lumen of the vessel, restricting blood flow. The reduced blood supply, particularly to distal tissues such as those in the lower limbs, results in ischemia. Over time, this can cause tissue damage, delayed healing, and in severe cases, necrosis. These vascular changes form the underlying mechanism of both microvascular and macrovascular complications associated with chronic hyperglycemia.

2.5. Progression of Diabetic Foot:

Reduced blood flow due to vascular damage leads to ischemia, where the affected tissues receive less oxygen and nutrients than required. Over time, this results in tissue damage and eventual cell death (necrosis). The skin becomes dry and loses its normal regenerative ability, leading to hardening and reduced flexibility. Because of this, even minor pressure or friction can cause cracks or small wounds. At the same time, poor circulation delays healing, allowing these small injuries to persist and worsen. [1]

In parallel, nerve damage (neuropathy) develops due to prolonged metabolic stress. Sensory nerve damage reduces pain perception, so injuries often go unnoticed, while motor nerve involvement can alter foot mechanics and increase pressure points. This combination leads to the formation of

calluses, cracks, and wounds. With continued exposure to external contaminants, these wounds are highly susceptible to infection. If left untreated, the combined effects of ischemia, infection, and tissue damage can progress to ulceration and eventually gangrene, which in severe cases may require amputation. [1]

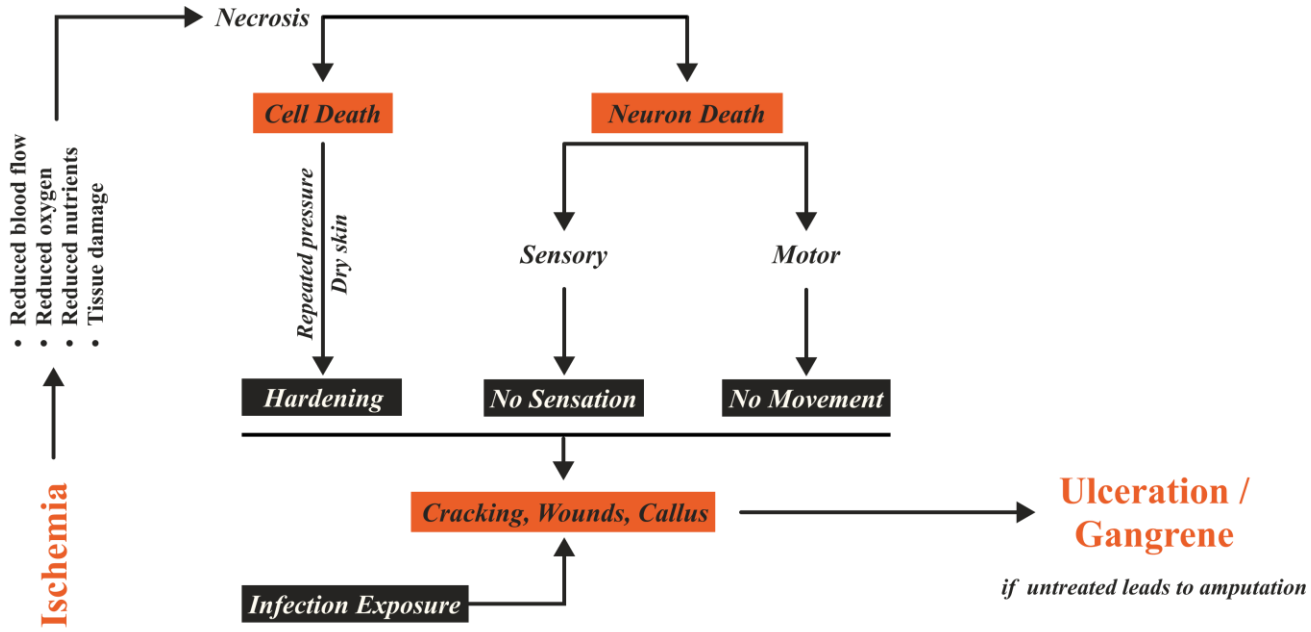

Figure 5:- Progression of ischemia and neuropathy leading to tissue damage, ulceration, and gangrene in diabetic foot conditions.

2.6. Electrical Equivalence Modelling of the Foot

TPBM The electrical behaviour of the foot can be represented using a simplified equivalent circuit that reflects its layered structure and composition. The outermost layer of the skin, especially the stratum corneum, is relatively dry and acts as a high-resistance element. Beneath this, the epidermis, dermis, and subcutaneous tissues contain ionic fluids (intra- and extracellular fluids), which provide conductive paths and therefore behave as resistive components. At the cellular level, the lipid bilayer of cell membranes does not allow direct current flow but can store charge, thereby introducing capacitive behaviour. [3]

To model this electrically, the foot is commonly represented as a parallel RC network in series with an additional resistance. The parallel combination consists of a resistance R_1 (representing tissue fluids and conductive pathways) and a capacitance C (representing cell membranes). This parallel RC branch captures the frequency-dependent behaviour of biological tissue—at low frequencies, the capacitive reactance is high, so current mainly flows through resistive paths; at higher frequencies, the

capacitive path becomes more significant, allowing current to pass through cell membranes. In series with this, an additional resistance R_2 represents deeper tissue layers and bulk fluid resistance. [5]

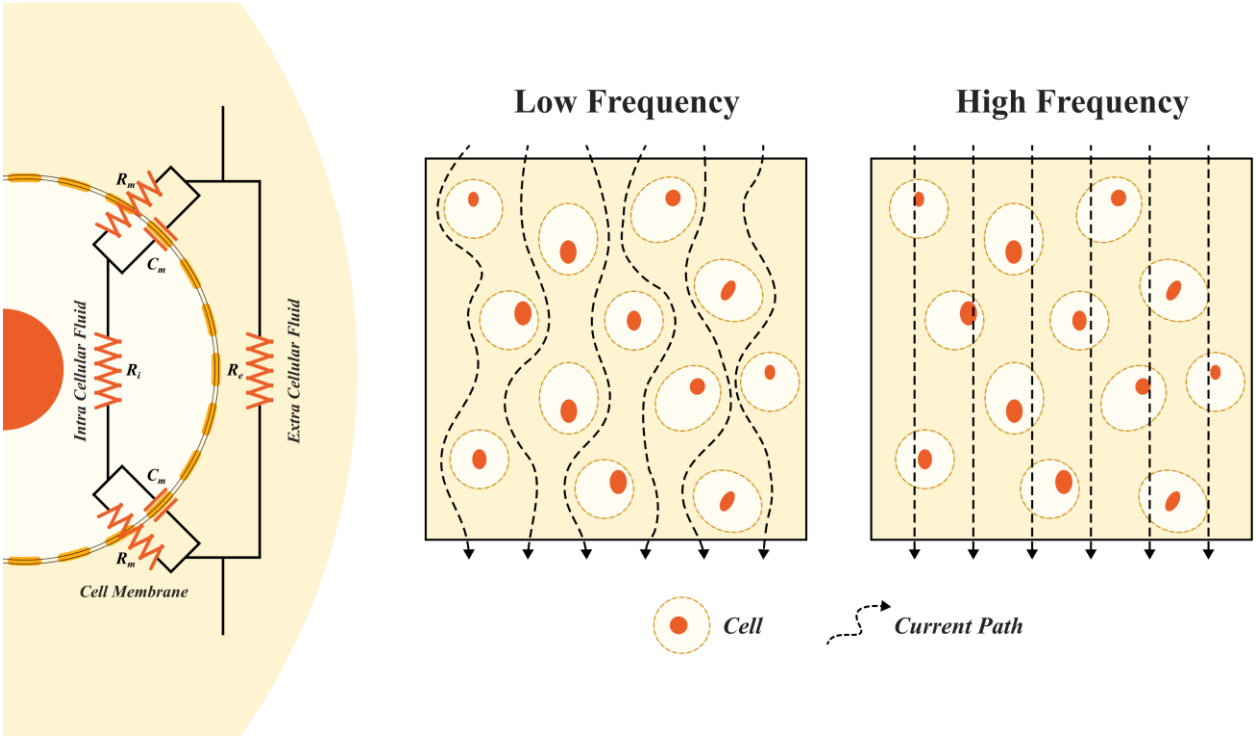

Figure 6:- Electrical representation of biological tissue showing cell membrane capacitance and resistive pathways, along with frequency-dependent current flow through extracellular and intracellular regions.

This model explains why foot impedance varies with frequency, which is the fundamental principle behind bio-impedance measurements. At lower frequencies, impedance is dominated by resistive components (mainly the outer skin layer), while at higher frequencies, capacitive effects reduce overall impedance as current penetrates deeper into the tissue. Such an RC-based representation is essential for interpreting impedance spectra and forms the basis for analyzing variations in foot tissue properties. [4]

2.7. Effect of Ischemia and Tissue Degeneration on Foot Impedance

As diabetic complications progress, vascular impairment reduces blood flow to the foot, leading to ischemia and inadequate oxygen and nutrient supply. This chronic ischemic condition gradually results in tissue damage and eventual cell death (necrosis). One of the key structural changes during this process is the loss of viable cell membranes. Since intact cell membranes behave as

capacitive elements (due to their lipid bilayer structure), their degradation directly reduces the overall capacitance ((C)) of the tissue.

From an electrical perspective, this alters the equivalent RC model of the foot. In healthy tissue, the parallel combination of resistance ((R_1)) and capacitance ((C)) allows current to pass through both resistive (fluid) and capacitive (membrane) pathways, especially at higher frequencies. However, as cell membranes break down due to necrosis, the capacitive pathway weakens, effectively reducing (C). This increases the overall impedance, particularly in the frequency ranges where capacitive effects are significant. In addition, ischemia also reduces fluid content and alters ionic distribution, which can further increase the resistive component.

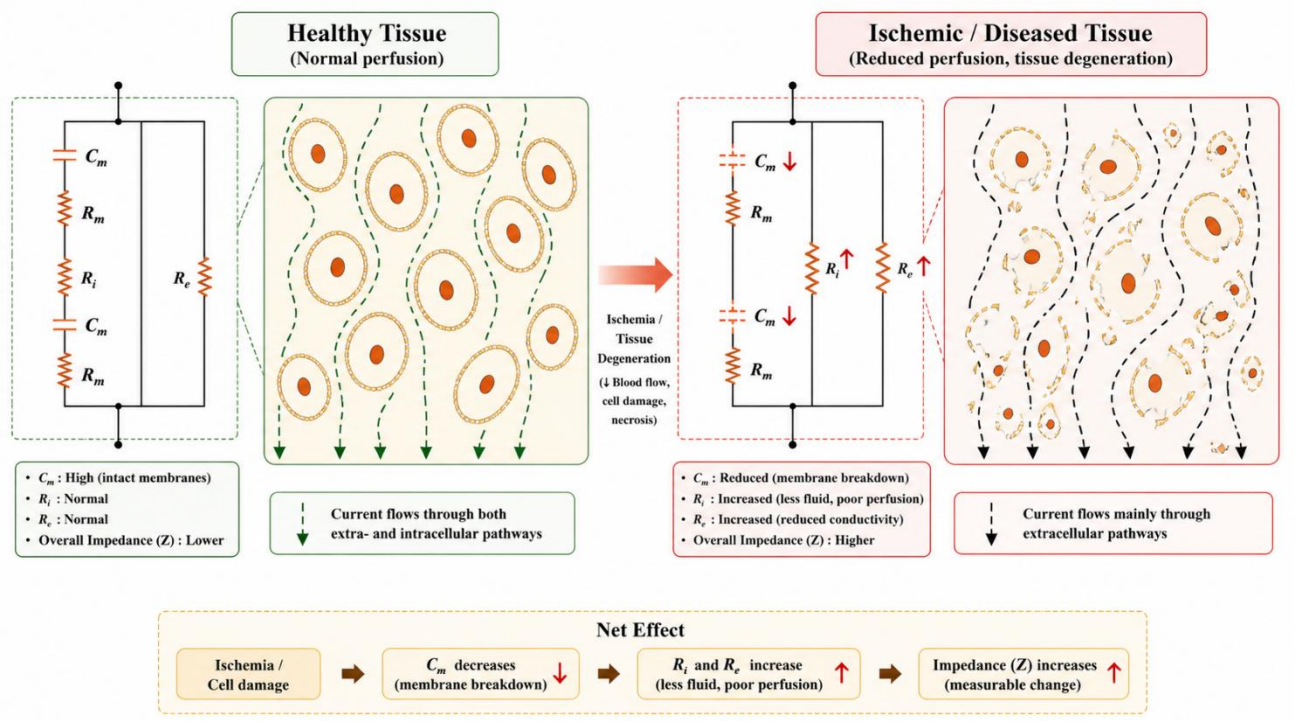

Figure 7:- Comparative schematic illustrating electrical changes in healthy and ischemic tissue, showing reduction in cell membrane capacitance and increase in resistive components leading to higher overall impedance.

Therefore, the observed increase in impedance in affected foot regions can be attributed to a combination of reduced capacitance (due to loss of cell membrane integrity) and increased resistance (due to reduced perfusion and fluid content). This relationship forms the underlying basis for using bio-impedance measurements as a means to study and track tissue-level changes associated with diabetic foot conditions, without directly implying diagnostic capability.

2.8. Bio-Impedance Measurement in Biological Tissue

Bio-impedance measurement involves the application of a small alternating current (AC) signal to biological tissue and observing the resulting voltage response to determine its electrical properties. Since biological tissues are composed of fluids, cells, and membranes, they exhibit both resistive and capacitive characteristics. When an AC signal is applied, the measured impedance is therefore complex in nature, consisting of real (resistive) and imaginary (capacitive) components. These components can be used to derive parameters such as impedance magnitude and phase. [3]

A key aspect of bio-impedance measurement is the use of frequency variation. At lower frequencies, current primarily flows through extracellular pathways due to the high impedance of cell membranes. At higher frequencies, the capacitive reactance of cell membranes decreases, allowing current to penetrate intracellular regions. This frequency-dependent behaviour enables the characterization of different tissue properties and depths. As a result, multi-frequency impedance analysis is widely used to study structural and physiological variations in biological tissues. [4]

2.9. Bio-Impedance Studies in Foot and Diabetic Conditions

Previous studies have explored the use of bio-impedance techniques for assessing tissue characteristics under both normal and pathological conditions. It has been observed that impedance values vary based on factors such as tissue composition, hydration level, and structural integrity. In diabetic conditions, physiological changes such as reduced blood flow, neuropathy, and tissue degradation influence these electrical properties, resulting in measurable variations in impedance. [2]

In the context of foot-based measurements, impedance is also influenced by mechanical factors such as pressure distribution. Regions of the foot that experience higher pressure—such as the heel, metatarsal heads, and toe regions—are more prone to structural and vascular changes. These areas are clinically significant as they are more susceptible to ulcer formation. Therefore, several studies have focused on localized impedance measurements, indicating that spatial variation across the foot can provide meaningful insight into underlying tissue conditions. This highlights the importance of selecting measurement points based on pressure distribution rather than arbitrary placement.[2]

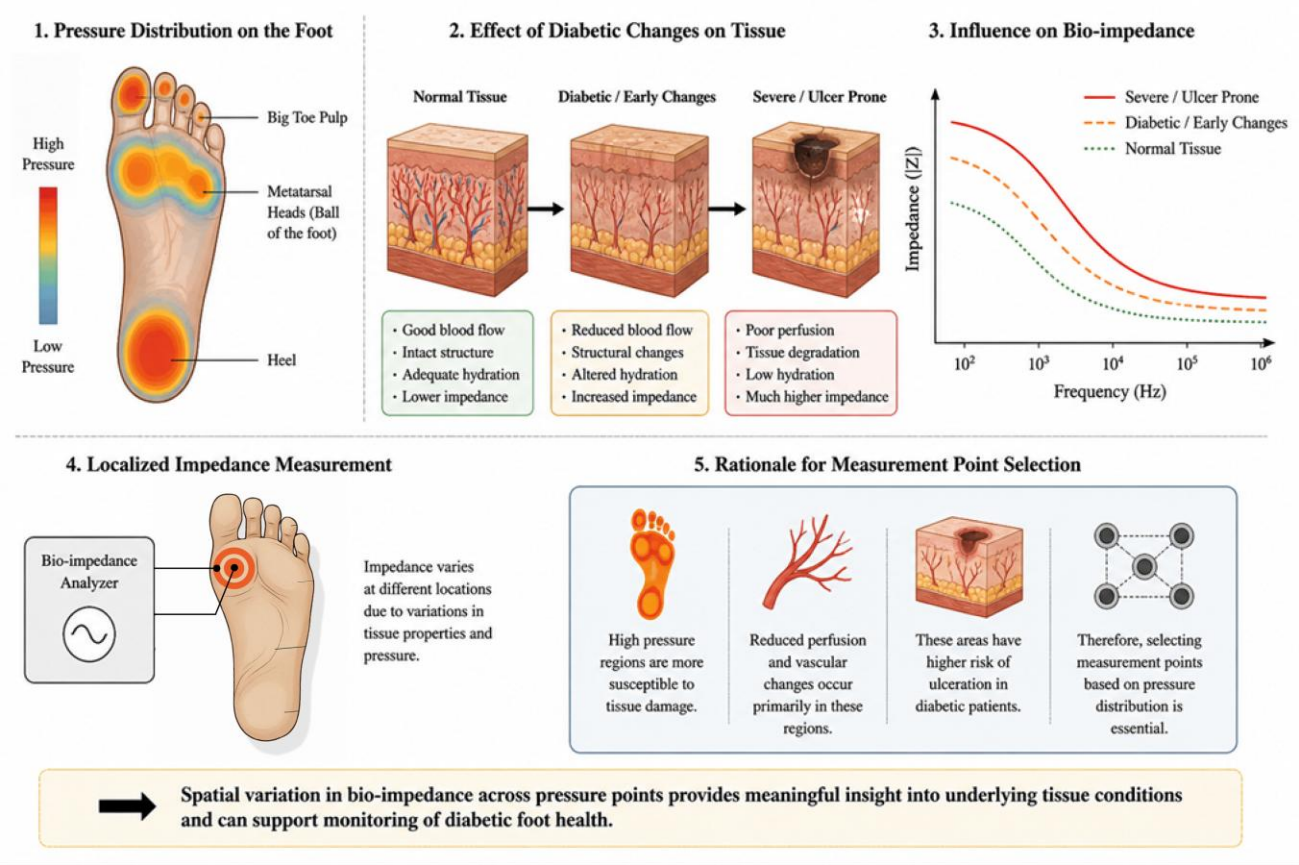

Figure 8:- Conceptual illustration of pressure-based foot regions and their influence on localized bio-impedance, highlighting how structural and vascular changes in diabetic conditions lead to measurable variations across different foot locations.

2.10. Existing Measurement Systems and Limitations

Several systems have been developed for measuring bio-impedance, ranging from laboratory-grade instruments to wearable prototypes. Devices such as LCR meters and impedance analyzers provide accurate measurements across a wide frequency range; however, they are typically bulky, expensive, and not suitable for portable or continuous use. On the other hand, wearable systems such as sensor-integrated socks offer a more practical approach for monitoring, but often have limitations in terms of measurement flexibility, electrode placement control, and frequency sweep capability.

Additionally, many existing systems are designed for generalized measurements rather than localized analysis at specific points of interest on the foot. There is limited availability of compact systems that can perform controlled, multi-frequency impedance measurements across multiple foot locations in a structured manner. These limitations highlight the need for a system that balances portability, measurement accuracy, and spatial resolution.tudies have explored the use of bio-

impedance techniques for assessing tissue characteristics under both normal and pathological conditions. [2,8,9]

2.11. Research Gap and Motivation

From the existing literature, it can be observed that while bio-impedance has been widely studied for tissue characterization, there is a lack of systems that focus on localized, multi-point impedance measurement of the foot using a controlled frequency sweep approach. Most existing solutions either emphasize clinical accuracy with bulky equipment or focus on wearable convenience with limited measurement control.

Furthermore, there is limited work that combines multi-location electrode measurement, frequency-dependent analysis, and portable embedded implementation into a single system. This creates an opportunity to explore a device that can systematically study impedance variations across different regions of the foot while maintaining simplicity and portability. The motivation of this work is therefore to experimentally investigate these variations using a structured and controlled measurement setup. [2,8,9]

2.12. Proposed Work

Based on the understanding developed through the literature, this work focuses on the design and development of a portable bio-impedance measurement system for foot-based analysis. The system is intended to measure impedance at multiple predefined locations on the foot using an array of electrodes integrated into a dedicated foot interface.

The electrode placement is specifically designed to target high-pressure regions of the foot, such as the heel and metatarsal areas, where tissue changes are more likely to occur. A frequency sweep-based measurement approach is implemented using an impedance converter integrated circuit, controlled by an embedded system for automated operation. The system incorporates features such as electrode switching, automated calibration, and real-time data acquisition. The collected impedance data is processed and visualized through a software interface to generate impedance versus frequency plots for different regions of the foot. This setup enables a structured investigation of spatial and frequency-dependent impedance variations.

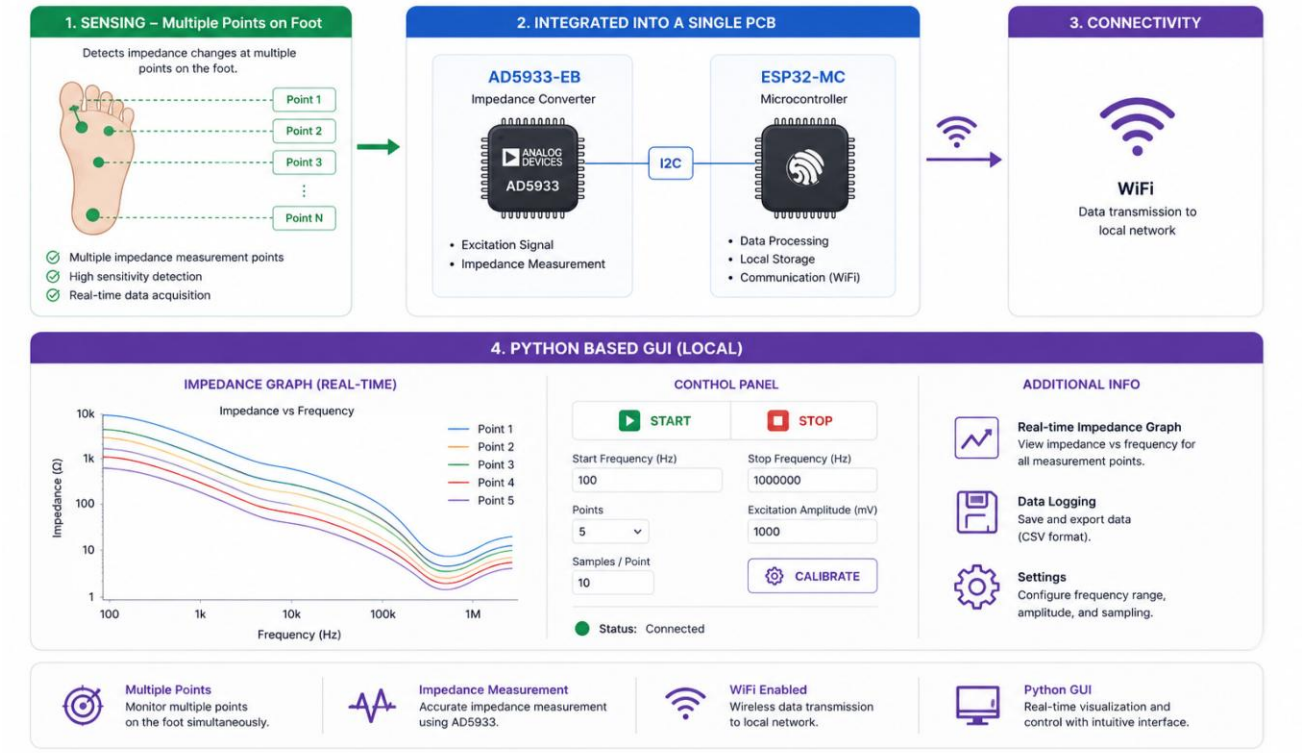

Figure 9:- High level integrated system architecture of the device.

Chapter 3: Materials and Methods

3.1. System Overview

The proposed system is a portable multi-point foot bio-impedance measurement platform designed to acquire impedance data from different regions of the foot. The system comprises an electrode interface, analog front-end circuitry, an impedance measurement unit, and a microcontroller-based control system. Multiple electrode points are selected using multiplexers to enable sequential measurements across predefined foot locations. The system also incorporates multiple calibration and feedback configurations to accommodate a wide range of impedance values.

An impedance converter IC (AD5934) is utilized to perform frequency sweep measurements, while an embedded microcontroller (ESP32-WROOM-32) controls the overall measurement process, including parameter configuration, electrode selection, and data acquisition. The measured data is transmitted to a software interface for visualization and analysis in the form of impedance spectra and spatial representations.

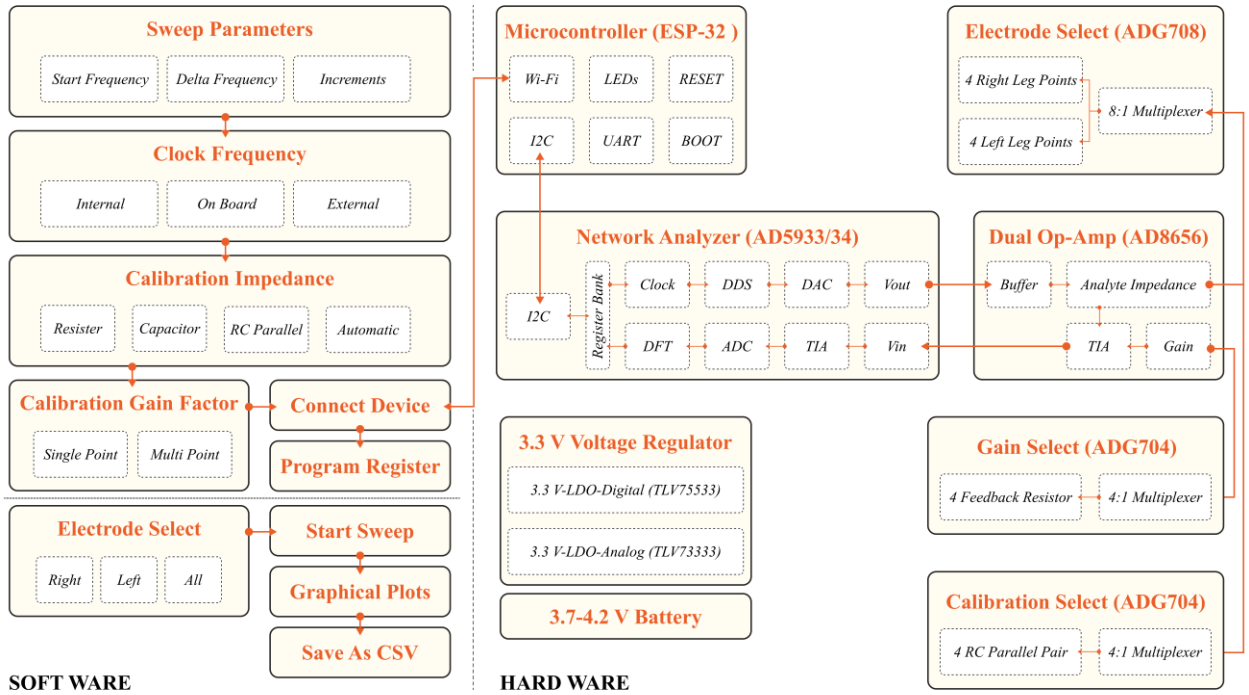

Figure 10:- Block diagram of the proposed multi-point foot bio-impedance measurement system illustrating the integration of electrode selection, impedance analysis (AD5933), signal conditioning, microcontroller control (ESP32), calibration network, and software-based data acquisition and visualization.

3.2. System Architecture

The system operates by applying an AC excitation signal to the foot and measuring the resulting electrical response at selected electrode locations. All electrode points are connected to the measurement system; however, at any given time, only one electrode is actively selected through a multiplexer for measurement.

The impedance measurement IC generates the excitation signal, which is applied to the tissue. The response from the selected electrode point is routed through a single multiplexer, allowing sequential measurement across multiple predefined locations without changing the physical setup. This approach simplifies the hardware design while enabling localized impedance acquisition.

The microcontroller communicates with the impedance analyzer via an I^2C interface to configure sweep parameters such as start frequency, frequency increment, and number of measurement points. It also controls the multiplexer using GPIO signals to select the desired electrode location. The measured impedance data is then processed and transmitted to the software interface for visualization and analysis.

3.3. Hardware Design

The hardware design of the proposed system consists of an electrode interface, signal-conditioning circuitry, an impedance measurement unit, electrode selection circuitry, calibration and gain selection networks, a microcontroller unit, and a regulated power supply. These components are integrated to form a compact and portable platform for bio-impedance measurement of the foot. The electrode interface provides contact with the tissue, enabling the application of an excitation signal and acquisition of the response. The signal is then processed through an analog front-end for buffering and amplification to maintain signal integrity and reduce noise. The impedance measurement unit performs frequency sweep-based analysis to characterize the electrical properties of the tissue.

A multiplexing approach is used to enable multi-point measurements using a single measurement channel. All electrodes are connected to the system, but only one electrode is selected at a time through controlled switching, allowing sequential measurements across different foot locations. Calibration and gain selection networks are included to handle variations in impedance and improve measurement accuracy. The microcontroller controls the overall operation, including parameter configuration, electrode selection, and data acquisition, while also managing communication with the software

interface. A regulated power supply ensures stable operation of both analog and digital sections of the system.

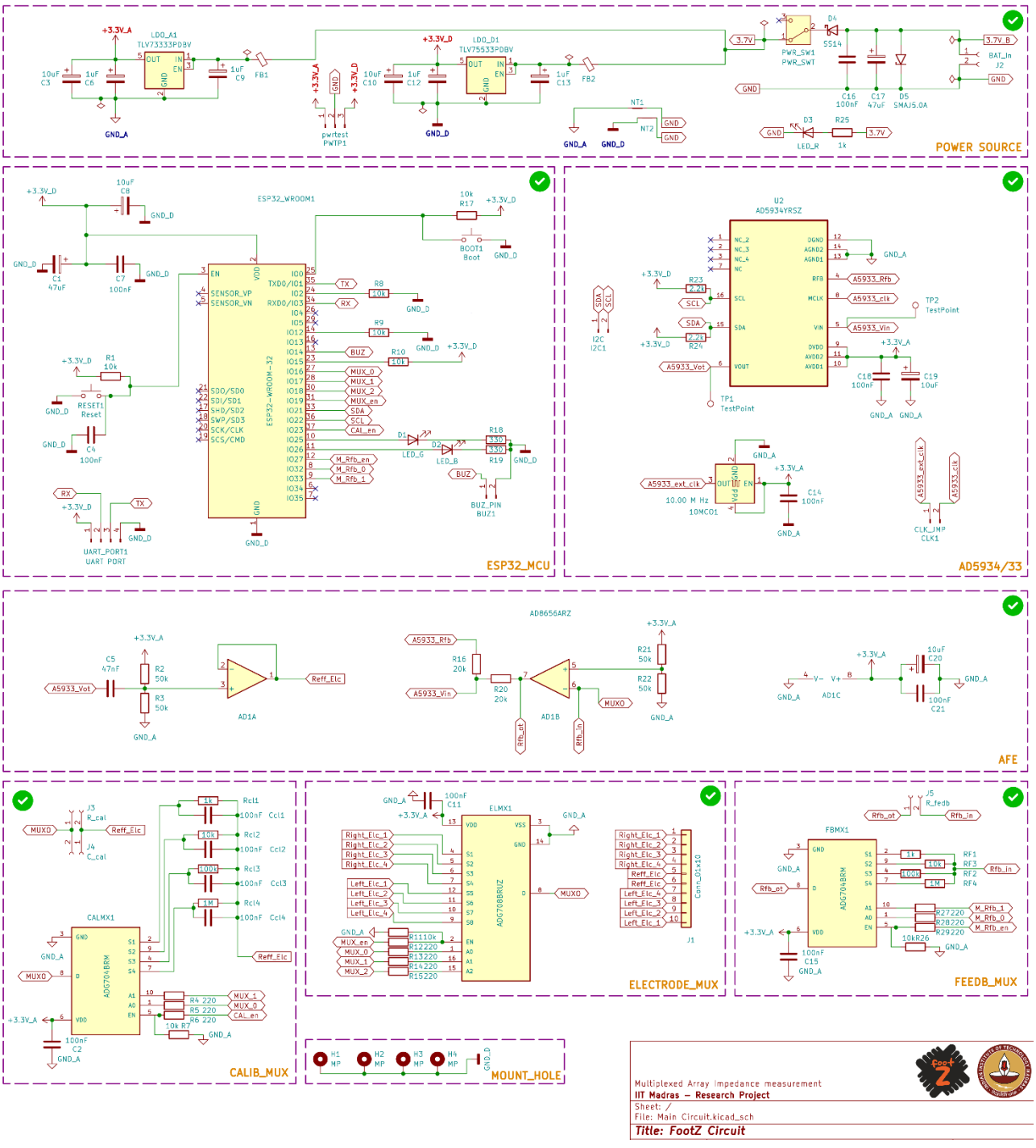

Figure 11:- Detailed hardware schematic of the proposed multi-point foot bio-impedance measurement system, designed using KiCad, showing integration of electrode interface, multiplexing, impedance measurement (AD5934), signal conditioning, microcontroller control

3.3.1. Electrode Interface and Foot Platform

The electrode interface consists of multiple contact points arranged on a foot platform to enable localized impedance measurement. The electrodes are positioned at predefined high-pressure regions of the foot, such as the heel, metatarsal areas, and toe regions, where structural and vascular changes are more likely to occur. Eight electrodes are implemented to capture spatial variations in impedance, with four electrodes placed on each side of the foot platform to ensure coverage of key regions.

The foot platform is designed using SketchUp and fabricated using 3D printing to provide a stable and repeatable measurement setup. Circular PCB-based electrodes are used for impedance measurement, ensuring consistent electrical contact and ease of integration with the circuitry. All electrodes are electrically connected to the system; however, only one electrode is selected at a time through a multiplexing mechanism. This approach allows sequential data acquisition across multiple locations without requiring repositioning of the electrodes. The overall design of the electrode interface and foot platform ensures proper alignment, stable contact with the skin, and improved measurement reliability.

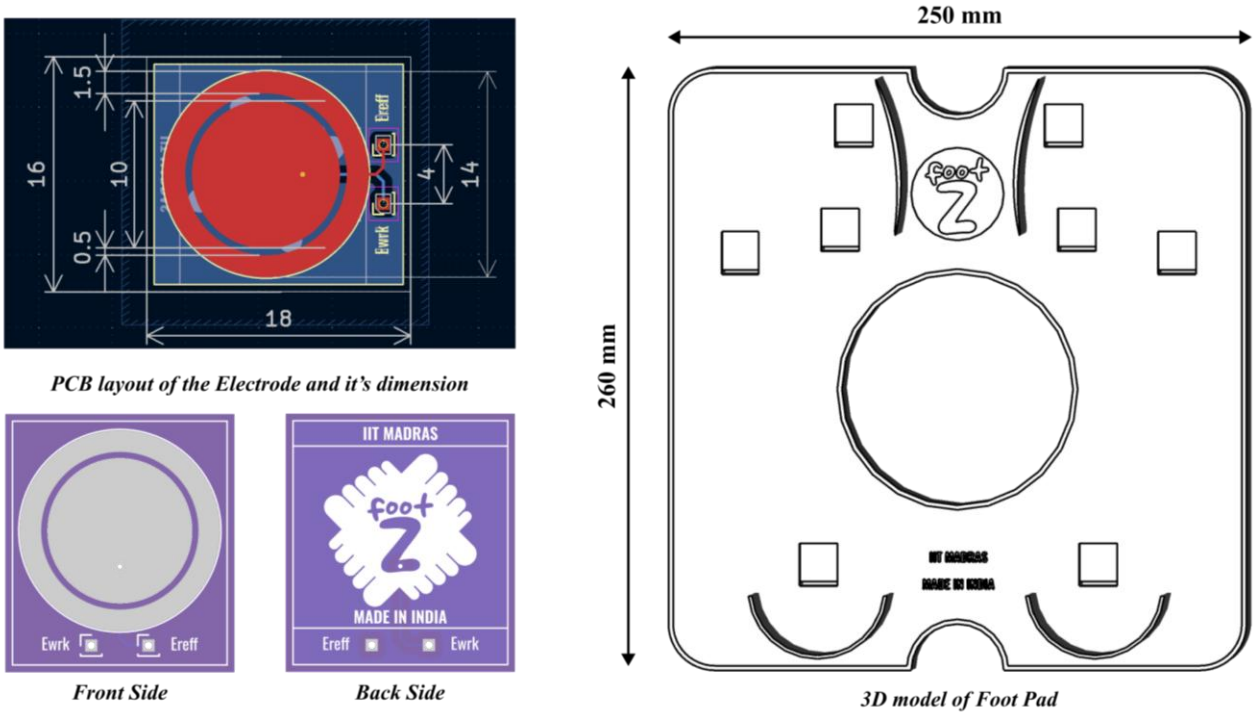

Figure 12:- Design and fabrication of the electrode interface and foot platform, showing the circular PCB-based electrode layout, electrode artwork, and the 3D-printed foot pad used for multi-point impedance measurements.

3.3.2. Electrode Electrode Selection Circuit (ADG708)

An analog multiplexer (ADG708) is employed for electrode selection within the system. The device enables routing of signals from one of the multiple electrode points to the impedance measurement circuit at a given time. This configuration allows the system to perform multi-point measurements using a single impedance measurement channel, thereby reducing hardware complexity while maintaining spatial resolution. The ADG708 is an 8:1 multiplexer, which aligns with the eight-electrode configuration of the system. At any given instance, only one electrode is connected to the measurement path, while the remaining electrodes remain isolated. The selection of the active electrode is controlled by the microcontroller (ESP32-WROOM-32) through digital control lines, ensuring precise and programmable switching. This approach enables efficient sequential scanning of electrode locations, minimizes signal interference between channels, and simplifies the overall circuit design.

3.3.3. Impedance Measurement Unit (AD5934)

The impedance measurement in the proposed system is performed using the AD5934 impedance converter IC, which integrates both signal generation and measurement functionalities. The device generates a sinusoidal excitation signal using an internal direct digital synthesizer (DDS), which is applied to the selected electrode and subsequently through the biological tissue.

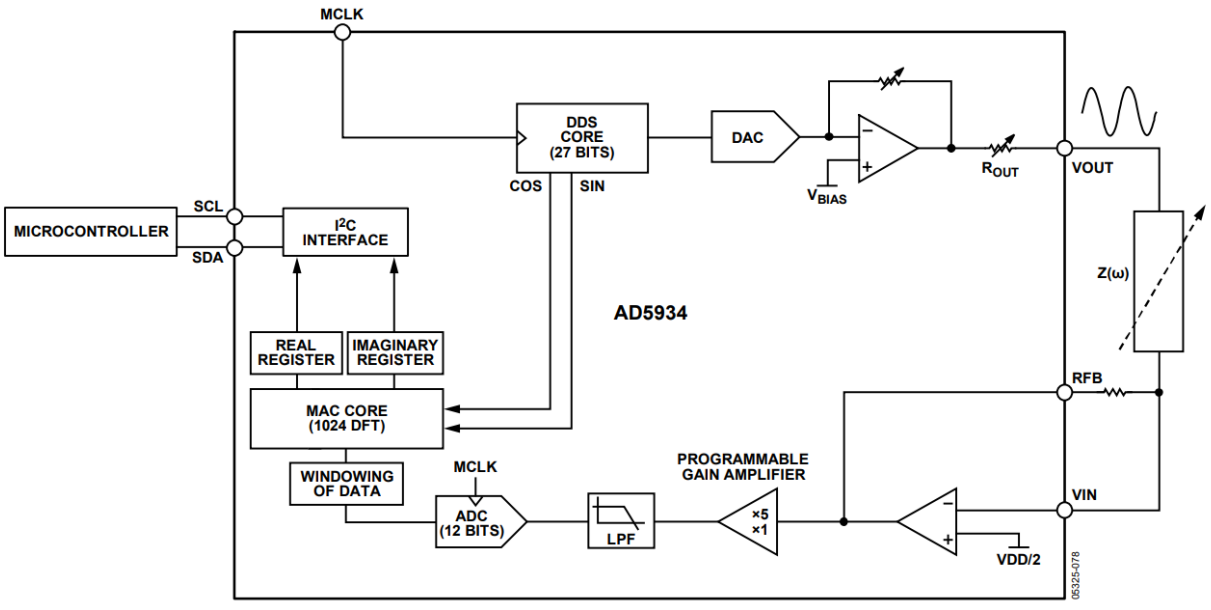

Figure 13:- Block diagram of the AD5934-based impedance spectroscopy measurement system.

The response signal from the tissue is converted into a voltage using an internal transimpedance amplifier (TIA) and digitized using an on-chip analog-to-digital converter (ADC). The AD5934 then performs a discrete Fourier transform (DFT) on the sampled data to obtain the real and imaginary components of the impedance. These components are used to calculate the magnitude and phase of the impedance.

The device supports programmable frequency sweep operation, allowing measurements over a specified frequency range by configuring parameters such as start frequency, frequency increment, and number of increments. This enables characterization of the electrical properties of the tissue across different frequencies. The AD5934 communicates with the microcontroller (ESP32-WROOM-32) via the I²C interface for configuration and data acquisition.

3.3.4. Analog Front End (Buffer and TIA using AD8656)

The The analog front-end (AFE) is implemented using the AD8656 dual operational amplifier to condition the signals between the electrode interface and the impedance measurement unit. The AFE consists of a buffering stage and a transimpedance amplifier (TIA) stage, which together ensure proper signal handling and measurement accuracy.

The buffer stage is used to isolate the electrode interface from the measurement circuitry, providing high input impedance and preventing loading effects on the biological tissue. This helps maintain signal integrity and ensures that the excitation signal is not distorted due to interface impedance variations.

The transimpedance amplifier (TIA) stage converts the current response from the tissue into a measurable voltage signal. Since the AD5934 measures voltage, the TIA plays a critical role in translating the current flowing through the tissue into a proportional voltage that can be accurately processed. The feedback components of the TIA determine the gain of the conversion and are selected based on the expected impedance range.

The use of a dual op-amp allows both buffering and current-to-voltage conversion to be implemented efficiently within a compact design. Overall, the analog front-end improves signal stability, reduces noise, and ensures reliable impedance measurements across different operating conditions.

3.3.5. Gain Selection Circuit (ADG704)

To accommodate a wide range of impedance values encountered in biological tissue, a gain selection mechanism is implemented using the ADG704 analog multiplexer. This allows dynamic switching between different feedback resistors in the transimpedance amplifier (TIA) stage of the analog front-end.

By selecting appropriate feedback resistor values, the system can adjust the gain of the TIA to match the impedance range of the measured tissue. This ensures that the output signal remains within the optimal input range of the AD5934, preventing signal saturation for low impedance values and improving sensitivity for higher impedance measurements.

The gain selection is controlled by the ESP32 microcontroller through digital control signals, enabling flexible and programmable adjustment of the measurement range. This approach enhances the dynamic range and accuracy of the system, allowing reliable impedance measurements across different conditions.

3.3.6. Calibration Network

To ensure accurate impedance measurement, a calibration network is incorporated into the system using known impedance elements such as precision resistors, capacitors, and RC combinations. These reference elements are connected to the measurement path through switching circuitry, allowing the system to perform calibration prior to actual measurements.

The calibration process is used to determine a gain factor, which is required to convert the raw real and imaginary values obtained from the AD5934 into accurate impedance values. By measuring known reference impedances, the system accounts for variations in the analog front-end, signal path, and measurement circuitry. The selection of calibration elements is controlled by the microcontroller, enabling automated calibration as part of the measurement sequence. This improves the reliability and repeatability of the system and ensures consistent performance across different operating conditions and impedance ranges.

3.3.7. Power Supply and Regulation

The system is powered using a rechargeable battery source in the range of 7.4 -8.4 V. Stable operation is ensured using low-dropout regulators (LDOs) to generate a regulated 3.3 V supply required for both analog and digital components.

Separate LDOs are employed for the analog and digital sections to minimize noise coupling and improve measurement accuracy. Proper decoupling capacitors are placed near critical components to reduce supply noise and ensure stable performance of the impedance measurement system.

3.3.8. Microcontroller Unit (ESP32-WROOM-32)

The ESP32-WROOM-32 microcontroller serves as the central control unit of the system, coordinating all measurement and switching operations. It communicates with the AD5934 impedance converter via the I²C interface to configure sweep parameters such as start frequency, frequency increment, and number of points, and to retrieve the measured real and imaginary data.

The microcontroller also controls the analog multiplexers (ADG708 and ADG704) through GPIO pins to perform electrode selection, gain switching, and calibration routing. A defined measurement sequence is implemented in firmware to initialize the system, perform calibration, sequentially scan electrode locations, and acquire data across the configured frequency range. The ESP32 then transmits the collected data to the external software interface via serial or wireless communication for visualization and storage.

3.4. Software Design

The software component of the proposed system consists of two main parts: the embedded firmware running on the ESP32 microcontroller and a host-side Python-based interface for data acquisition, processing, and visualization. The embedded firmware is responsible for controlling the impedance measurement process, while the Python script manages communication, data processing, storage, and graphical representation of the measured impedance.

The embedded system initializes the hardware components, including the AD5934 impedance converter and the multiplexing circuitry. It configures the measurement parameters such as start frequency, frequency increment, and number of frequency points for the sweep operation. The microcontroller controls the AD5934 via the I²C interface to generate the excitation signal and perform frequency sweep measurements. It also manages electrode selection by controlling the multiplexer through GPIO pins, enabling sequential measurement across different electrode locations.

The firmware implements a structured measurement sequence consisting of calibration and measurement phases. During calibration, a known reference impedance is connected to the system, and the AD5934 performs a frequency sweep to obtain real and imaginary values. These values are

used to determine a gain factor, which is required to convert raw measurement data into actual impedance values. After calibration, the system switches to measurement mode, where the selected electrode is connected, and impedance data is acquired across the configured frequency range. The real and imaginary components obtained from the AD5934 are transmitted to the host system through serial communication.

On the host side, a Python-based interface is used to communicate with the embedded system via a serial port. The script continuously reads incoming data, which consists of frequency, real, and imaginary components for each measurement point. The data is parsed and stored in structured form for further processing. A calibration step is performed in the software by computing the gain factor using the known reference resistance and the measured magnitude values. This gain factor is then applied to subsequent measurements to compute the actual impedance.

For each measurement, the Python script calculates the magnitude of the impedance using the real and imaginary components and then derives the impedance value using the calibration factor. The system supports multiple measurement rounds, where the user can specify different foot regions or electrode locations. The acquired data is stored in a CSV file with timestamped filenames, allowing organized storage and later analysis. The stored data includes frequency, real part, imaginary part, magnitude, and calculated impedance values.

The processed data is visualized using graphical plots, where impedance is plotted against frequency. Both linear and logarithmic scales are supported, with logarithmic scaling used to better represent the wide range of impedance values. The plotting interface allows comparison of multiple measurement sets, enabling analysis of impedance variation across different locations. The overall software workflow ensures synchronized operation between the embedded system and the host interface, providing a complete pipeline for impedance measurement, processing, and visualization.

3.5 Summary of Methodology

The proposed system integrates both hardware and software components to enable multi-point bio-impedance measurement of the foot. The hardware design provides a compact and configurable platform incorporating electrode selection, signal conditioning, impedance measurement, and calibration mechanisms, while the embedded firmware ensures controlled execution of measurement

sequences. The host-side software facilitates data acquisition, processing, and visualization, allowing interpretation of impedance variations across different foot locations.

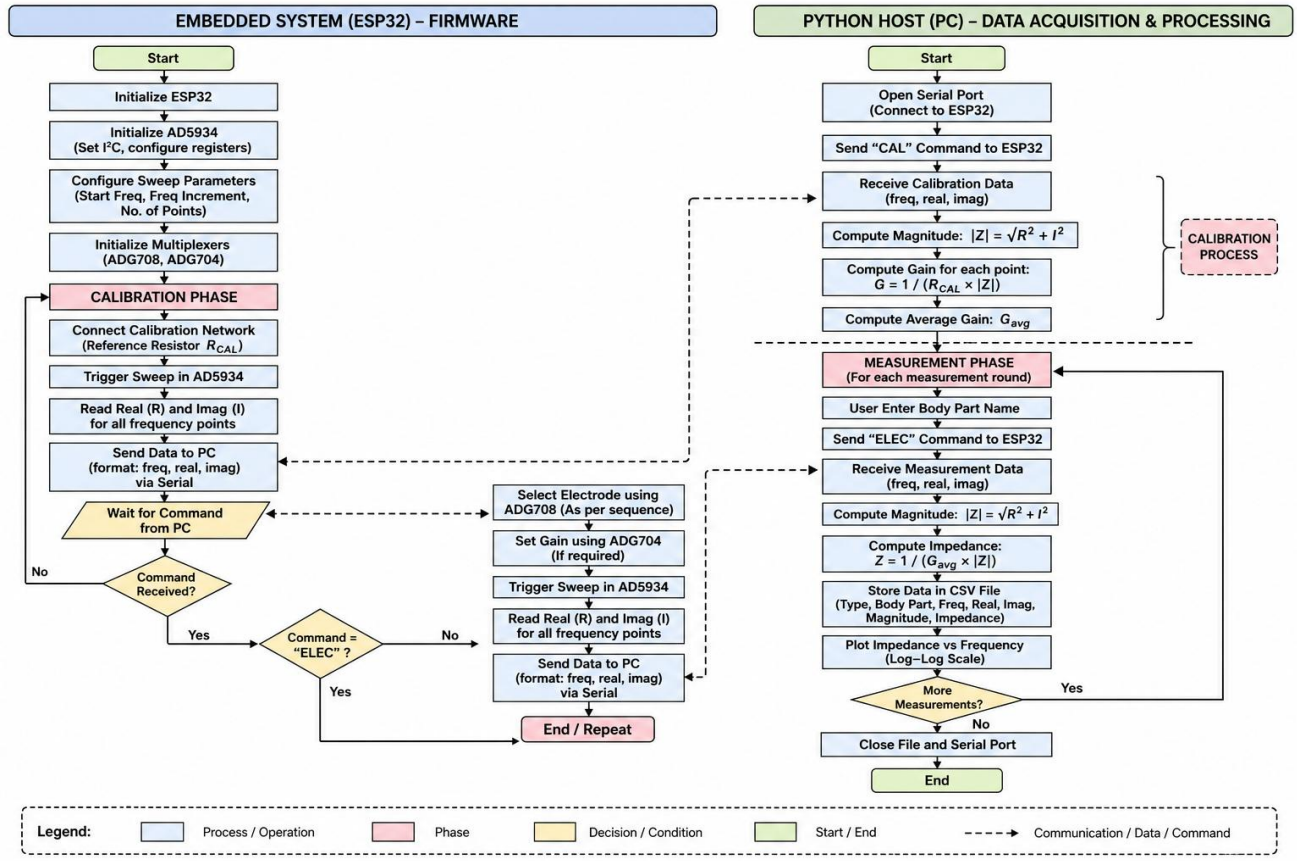

Figure 14:- Flowchart illustrating the embedded firmware (ESP32) and Python-based host software workflow, including system initialization, calibration process, multi-point impedance measurement, data acquisition, processing, and visualization.

The combined implementation enables reliable frequency-based impedance characterization with spatial resolution, using a single measurement channel through controlled switching. The design ensures flexibility in parameter configuration, adaptability to different impedance ranges, and repeatability of measurements. The methodology described in this chapter forms the basis for experimental evaluation, and the obtained results are presented and analyzed in the following chapter.

Chapter 4: Results and Discussions

4.1 Overview of Experimental Results

This chapter presents the results obtained from the developed multi-point foot bio-impedance measurement system. The results include the realization of the hardware system, electrode and foot platform implementation, impedance measurements across different locations, and visualization using the developed software interface. The measurements are analyzed primarily in terms of frequency-dependent trends and spatial variations across the foot. Due to partial calibration of the system, the results are interpreted based on relative impedance behavior rather than absolute impedance values.

4.2 Hardware Realization

The proposed system was successfully designed and implemented using a custom-designed printed circuit board (PCB). The PCB integrates all major components including the AD5934 impedance measurement unit, ESP32 microcontroller, analog front-end circuitry, multiplexing circuits, and calibration network. The hardware assembly demonstrates compact integration of measurement, control, and signal conditioning modules.

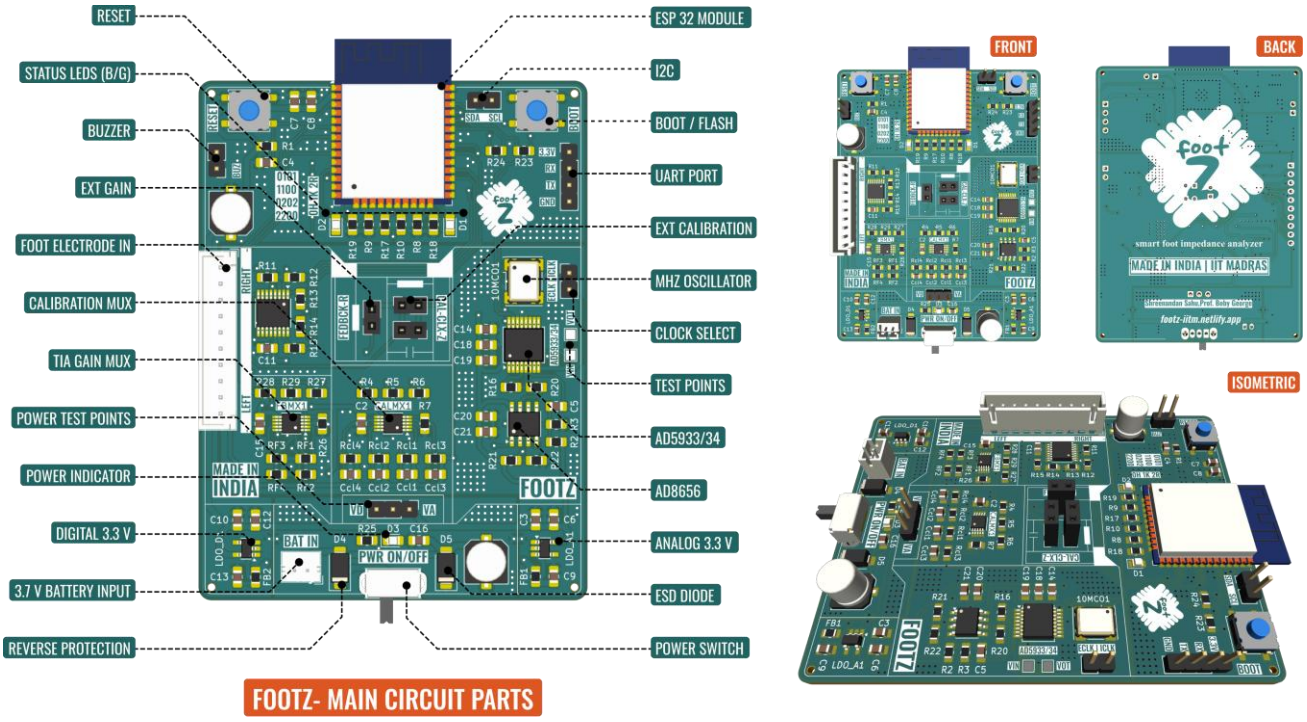

Figure 15:- Fabricated PCB and assembled hardware of the proposed foot bio-impedance measurement system, showing key components including the ESP32 microcontroller, AD5934 impedance analyzer, analog front-end, multiplexing circuitry, calibration network, and power management modules (front, back, and isometric views).

The complete system was tested for functionality, including communication between the microcontroller and impedance measurement unit, electrode switching, and data transmission. The hardware operated reliably, enabling controlled frequency sweep measurements and multi-point data acquisition.

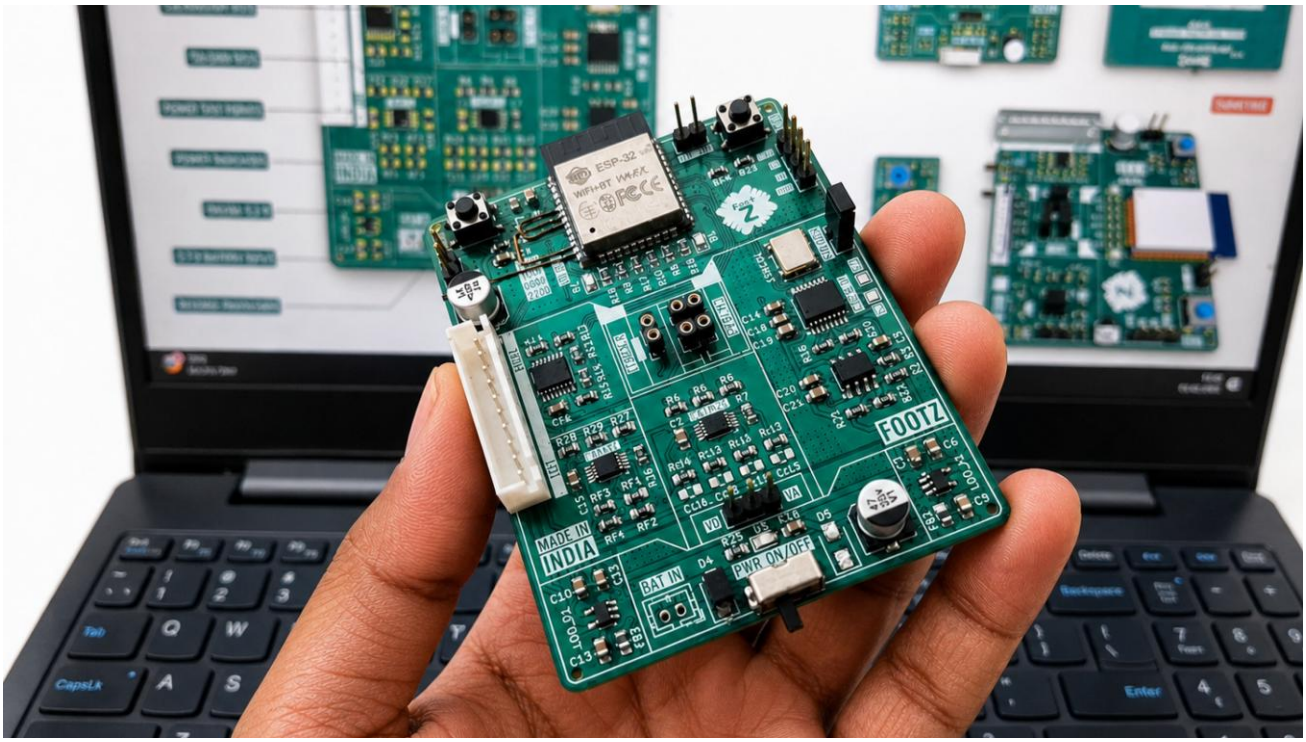

Figure 16:- Fabricated and assembled prototype of the proposed portable foot bio-impedance measurement device, showing the integrated ESP32 microcontroller, AD5934 impedance measurement unit, analog front-end and supporting circuitry.

4.3 Electrode and Foot Platform Implementation

The electrode interface was implemented using circular PCB-based electrodes mounted on a custom-designed foot platform. The platform was designed using SketchUp and fabricated using 3D printing to provide a stable and repeatable measurement setup. A total of eight electrodes were arranged, with four electrodes on each side of the platform, targeting high-pressure regions such as the heel, metatarsal areas, and toe regions.

The design ensures proper alignment and consistent contact with the skin, which is essential for reliable impedance measurements. The electrode configuration enables localized sensing, allowing comparison of impedance behavior across different regions of the foot.

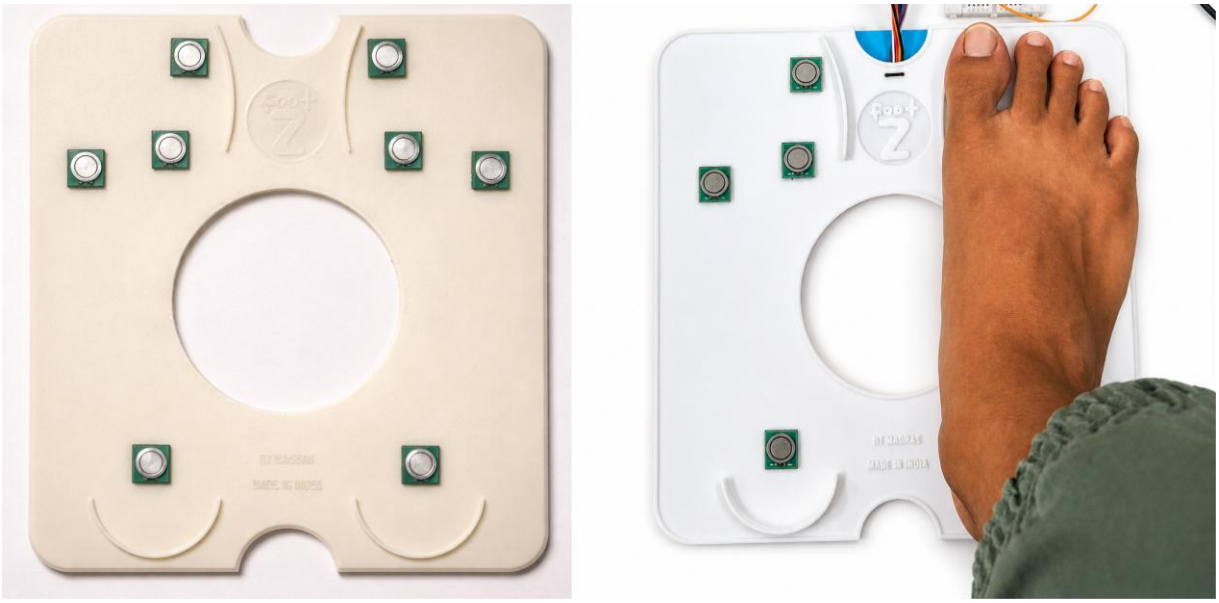

Figure 17:- 3D-printed foot platform with integrated circular PCB electrodes for multi-point impedance measurement, along with experimental setup showing foot placement for data acquisition.

4.4 Control Software and the GUI

The developed Python-based software interface enables real-time acquisition, processing, and visualization of impedance data obtained from the embedded system. The interface allows the user to configure measurement parameters such as start frequency, frequency step, and number of points, and facilitates communication with the ESP32 via serial communication. The raw data received from the device, consisting of real and imaginary components, is processed to compute impedance magnitude and phase across the frequency range.

On the embedded side, the ESP32 microcontroller manages the complete measurement process by configuring the AD5934 impedance converter, controlling electrode selection through multiplexing, and executing calibration and frequency sweep operations. It acquires the real and imaginary data from the AD5934 for each frequency point and transmits the data to the host system in a structured format. This coordinated operation ensures synchronized data acquisition across multiple electrode locations.

The software provides multiple visualization outputs, including plots of real and imaginary components, impedance magnitude, phase response, and Nyquist representation. These plots help in understanding the frequency-dependent behavior of the measured tissue and enable comparison across different measurement locations. The interface also supports structured data storage in CSV format for

further analysis. Overall, the software plays a crucial role in translating raw measurement data into interpretable graphical results, while the embedded system ensures accurate and controlled data acquisition, thereby enhancing the overall effectiveness of the proposed system.

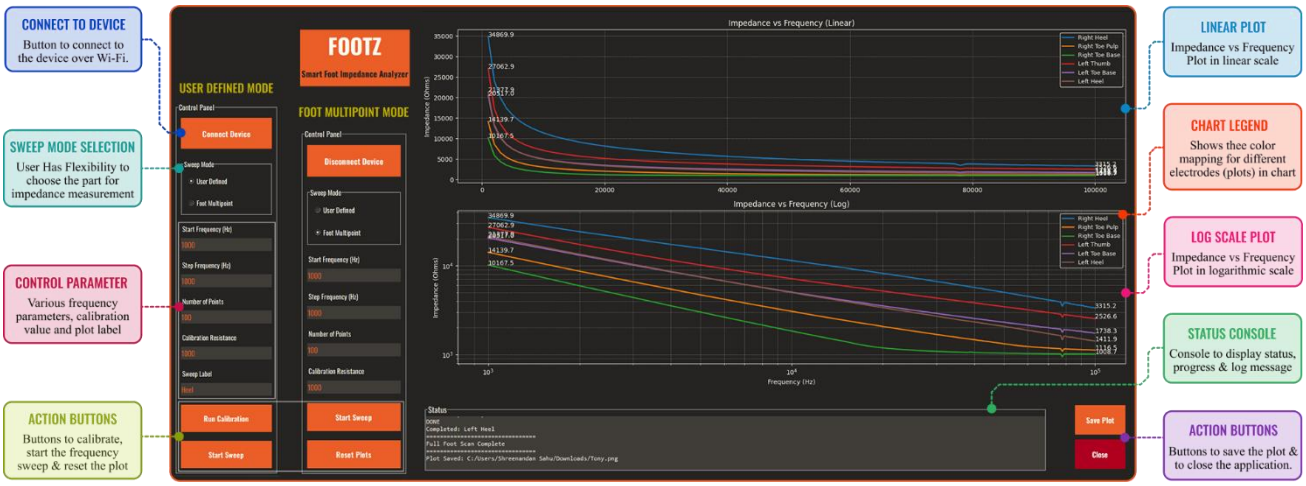

Figure 18:- FOOTZ: Real-Time Smart Foot Bioimpedance Analysis Interface with Multi-Region Impedance Visualization in Linear and Logarithmic Frequency Scales.

4.5 Impedance Measurement Results

4.5.1 Linear Scale Representation

The impedance measurements obtained from different electrode locations are plotted against frequency in linear scale. The plots show variation in impedance values across different regions of the foot. Although the absolute values are not fully calibrated, the relative differences between measurement locations are clearly observable. The linear scale representation provides an initial understanding of how impedance varies with frequency and location, highlighting the presence of spatial variation in the measured signals.

4.5.2 Logarithmic Scale Representation

To better visualize the variation over a wide frequency range, the impedance data is also represented in logarithmic scale. The log-scale plots clearly highlight the trends in impedance behavior across frequency and provide improved comparison between different measurement locations. The logarithmic representation enhances the visibility of changes at both low and high frequencies, making it easier to interpret the frequency-dependent characteristics of the measured signals.

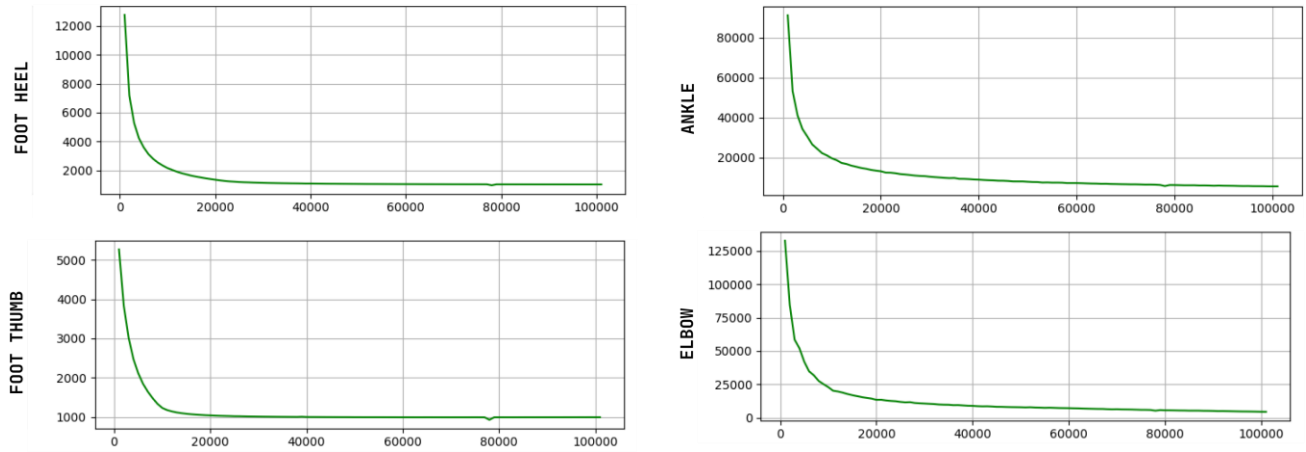

Figure 19:-Impedance trends of the device for different body parts for same frequency sweep plotted on linear scale

.

4.5.3 Spatial Variation Across Different types of Skin

The results demonstrate noticeable variation in impedance trends across different regions of the foot. Measurements were carried out at multiple locations including the big toe (thumb), toe region, mid-foot (arch), ankle region, and heel. Regions corresponding to higher pressure areas such as the heel and toe region exhibit impedance characteristics that differ from relatively lower pressure regions such as the mid-foot. These variations can be attributed to differences in tissue composition, hydration levels, vascularity, and pressure distribution across the foot.

The ability of the system to capture these spatial variations indicates that the multi-point measurement approach is effective in identifying localized differences in tissue properties. This reinforces the importance of region-specific impedance measurement rather than relying on a single-point assessment, as different areas of the foot exhibit distinct electrical behaviour

The results demonstrate expected frequency-dependent impedance behaviour across different body regions, with clear distinctions based on tissue properties. Calibration measurements validate system functionality, although full calibration across all frequencies is still in progress. Despite this, the observed trends are consistent with theoretical expectations, confirming the effectiveness of the system.

Figure 20:- Complete setup of the Portable device with all the components and parts marked

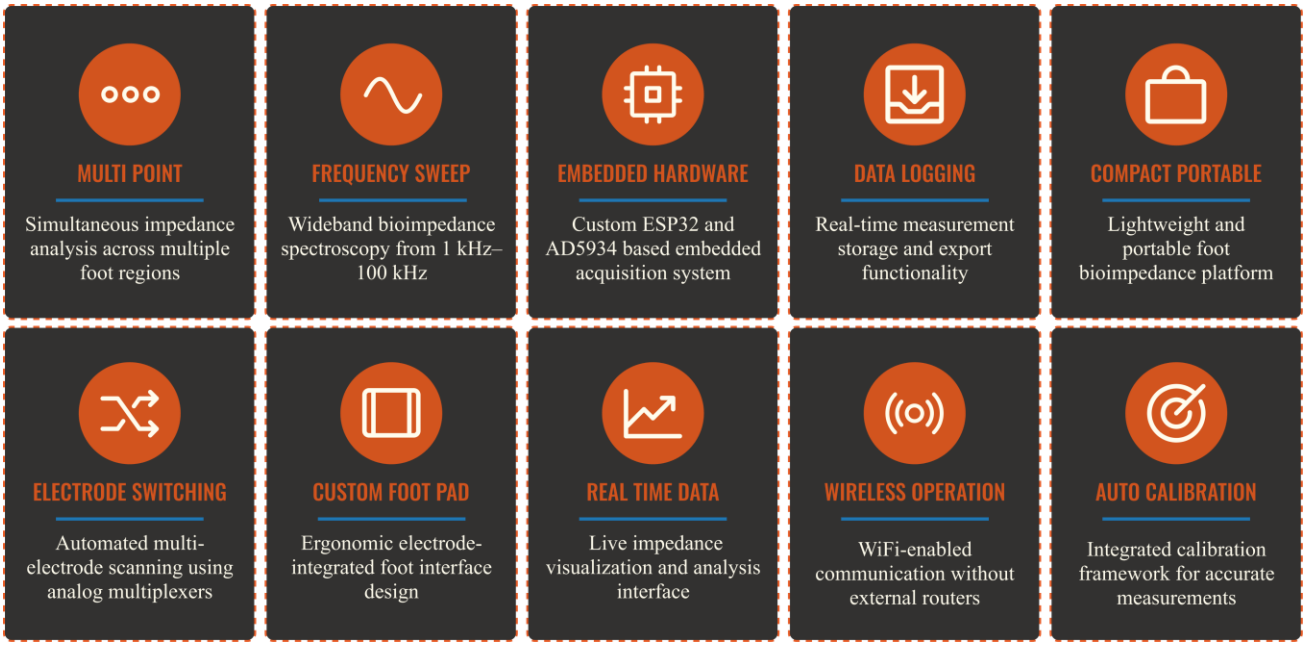

Figure 21:- All the features of the device and the system developed.

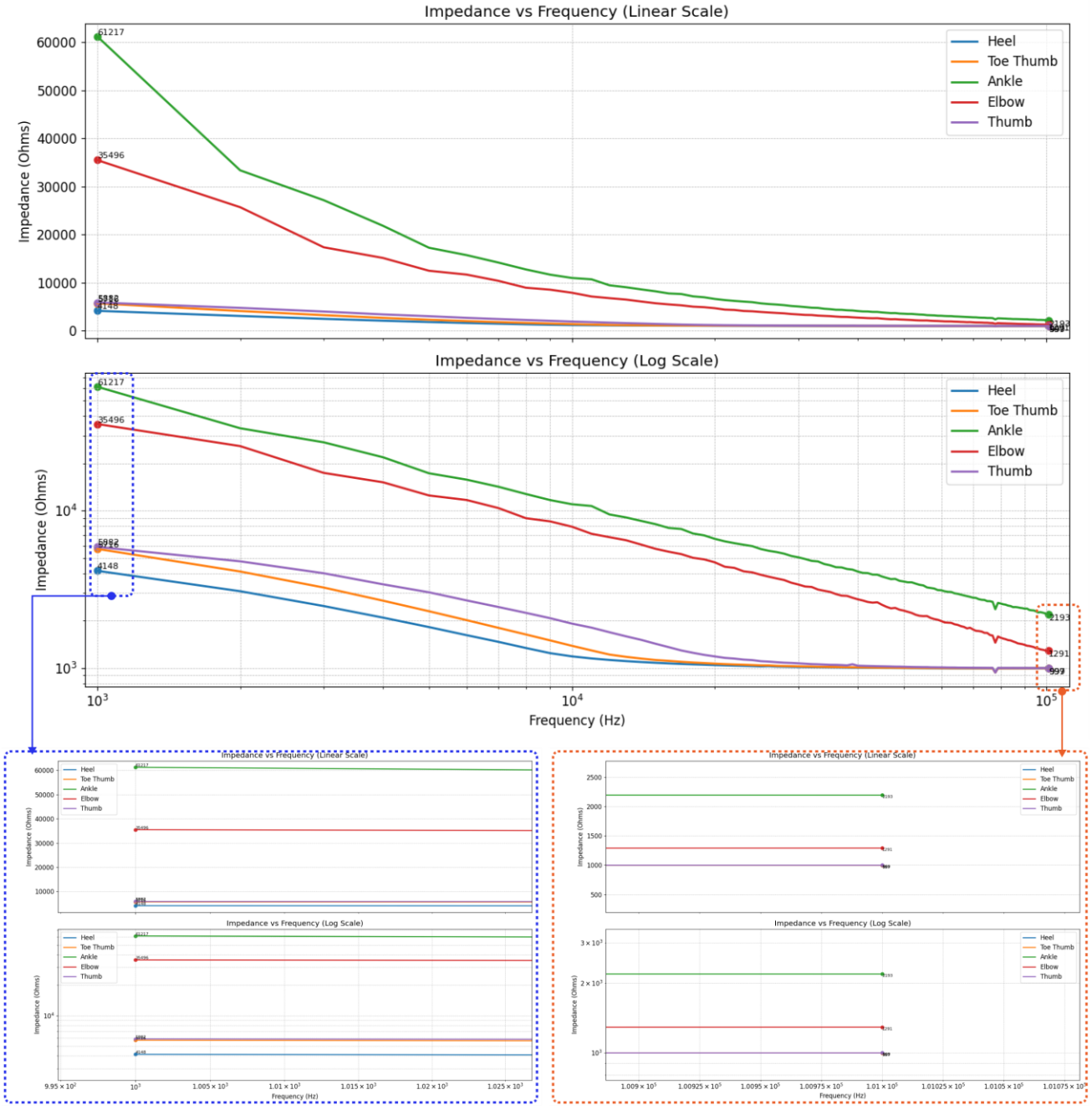

Figure 22:- Frequency-dependent impedance characteristics of multiple body regions. The linear plot (top) illustrates absolute impedance variation, while the logarithmic plot (bottom) emphasizes the dispersive behaviour and relative differences across tissues, indicating capacitive effects and structural heterogeneity.

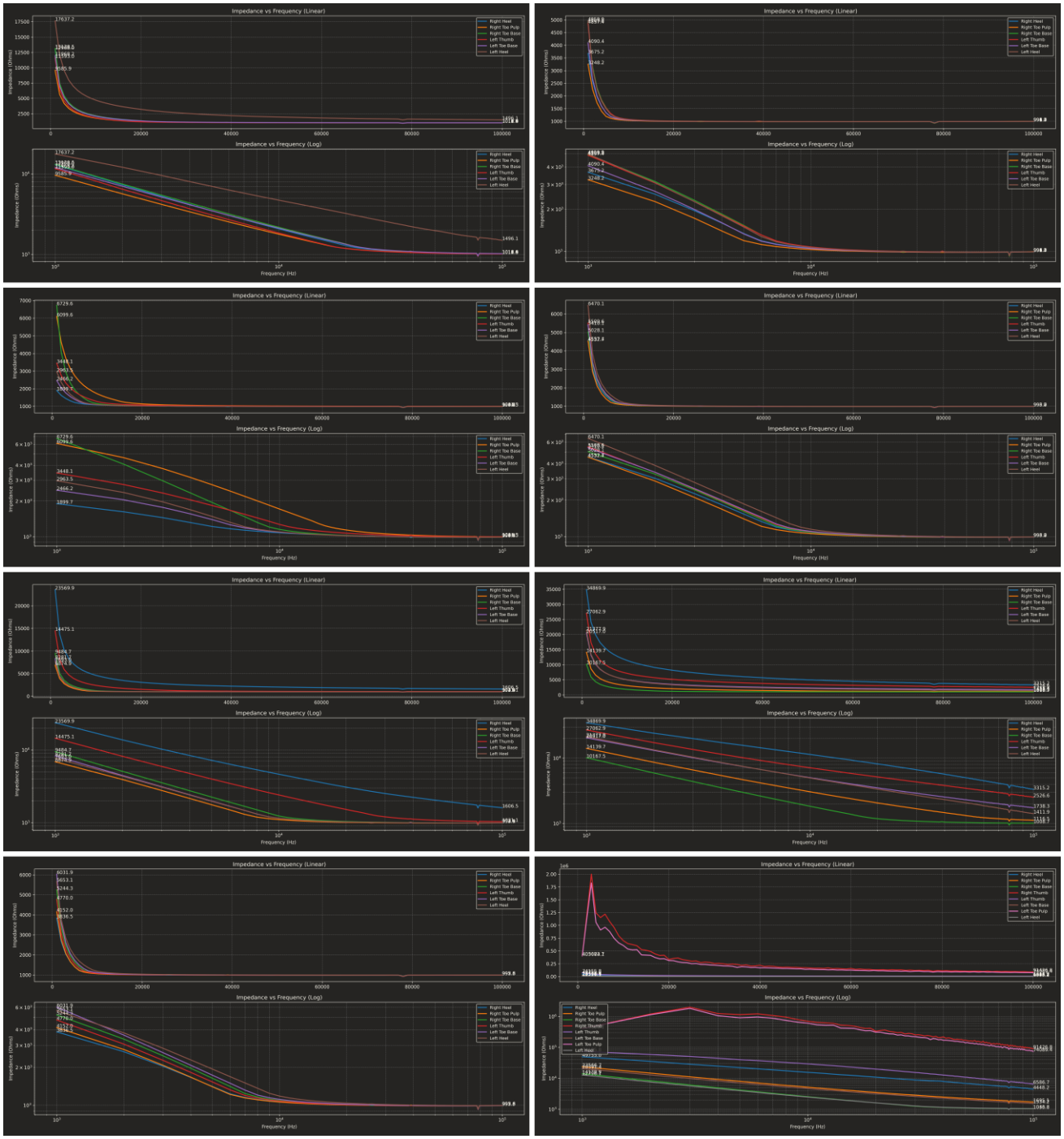

Figure 23:- Comparison of Impedance trends on different points on the foot of different people showing variation in the trends and values

Chapter 5: Conclusion

The preliminary experimental results demonstrate the capability of the developed bioimpedance measurement system to capture clear frequency-dependent impedance variations across different biological tissues. A frequency sweep ranging from 1 kHz to 100 kHz was performed using a single calibration configuration and fixed feedback resistance. Although this configuration is not ideal for accurately measuring a wide range of impedances, it was sufficient for validating the overall system behavior and identifying distinct impedance trends across different body regions.

The primary objective of the proposed system is foot bioimpedance analysis. However, during the preliminary testing stage, measurements were also conducted on multiple body regions including the ankle, elbow, heel, and thumb in order to evaluate the dynamic range and sensitivity of the system under varying skin and tissue conditions. The obtained plots clearly demonstrated distinguishable impedance characteristics for different body parts, confirming the ability of the system to detect variations in tissue composition and skin properties.

Across all measured regions, impedance was observed to decrease with increasing frequency, which is consistent with the expected electrical behavior of biological tissues. At lower frequencies, current conduction is predominantly limited to extracellular pathways due to the capacitive nature of cell membranes, resulting in higher impedance values. As frequency increases, the capacitive reactance decreases, allowing current to penetrate deeper tissue layers and reducing the overall impedance. At higher frequencies, the measured impedance gradually approaches a relatively stable resistive value, representing the dominant resistive conduction component of the tissue.

The variation in impedance among different body regions also matched expected physiological behavior. Regions such as the ankle and elbow exhibited comparatively higher impedance values due to thicker and rougher skin surfaces with a larger presence of dead cell layers, which reduce conductivity. In contrast, softer and better hydrated regions such as the thumb showed lower impedance values. The clear separation between these impedance trends demonstrates the sensitivity of the system to differences in biological tissue characteristics.

Open- and short-circuit measurements were additionally performed to validate the frontend response and overall measurement consistency. The open-circuit condition resulted in impedance values in the megaohm range, as expected in the absence of a conductive path. Similarly, the short-circuit condition produced a low and nearly constant impedance response throughout the frequency sweep. Although the measured short-circuit impedance did not ideally reach zero ohms, the stable

behavior indicates the presence of parasitic impedances, electrode resistance, and frontend non-idealities within the system.

It is important to note that the current measurements primarily represent trend validation rather than precise absolute impedance quantification. Since a single calibration resistor and fixed feedback resistance were used throughout the complete frequency sweep, certain impedance ranges may result in ADC saturation or signal amplitudes becoming too small for reliable acquisition. Consequently, while the absolute impedance values may not yet be fully accurate, the observed frequency-dependent trends and relative distinctions between different tissue measurements were clear, repeatable, and consistent with theoretical expectations. These results confirm the effective operation of the proposed hardware architecture and measurement methodology during the preliminary stage of development.

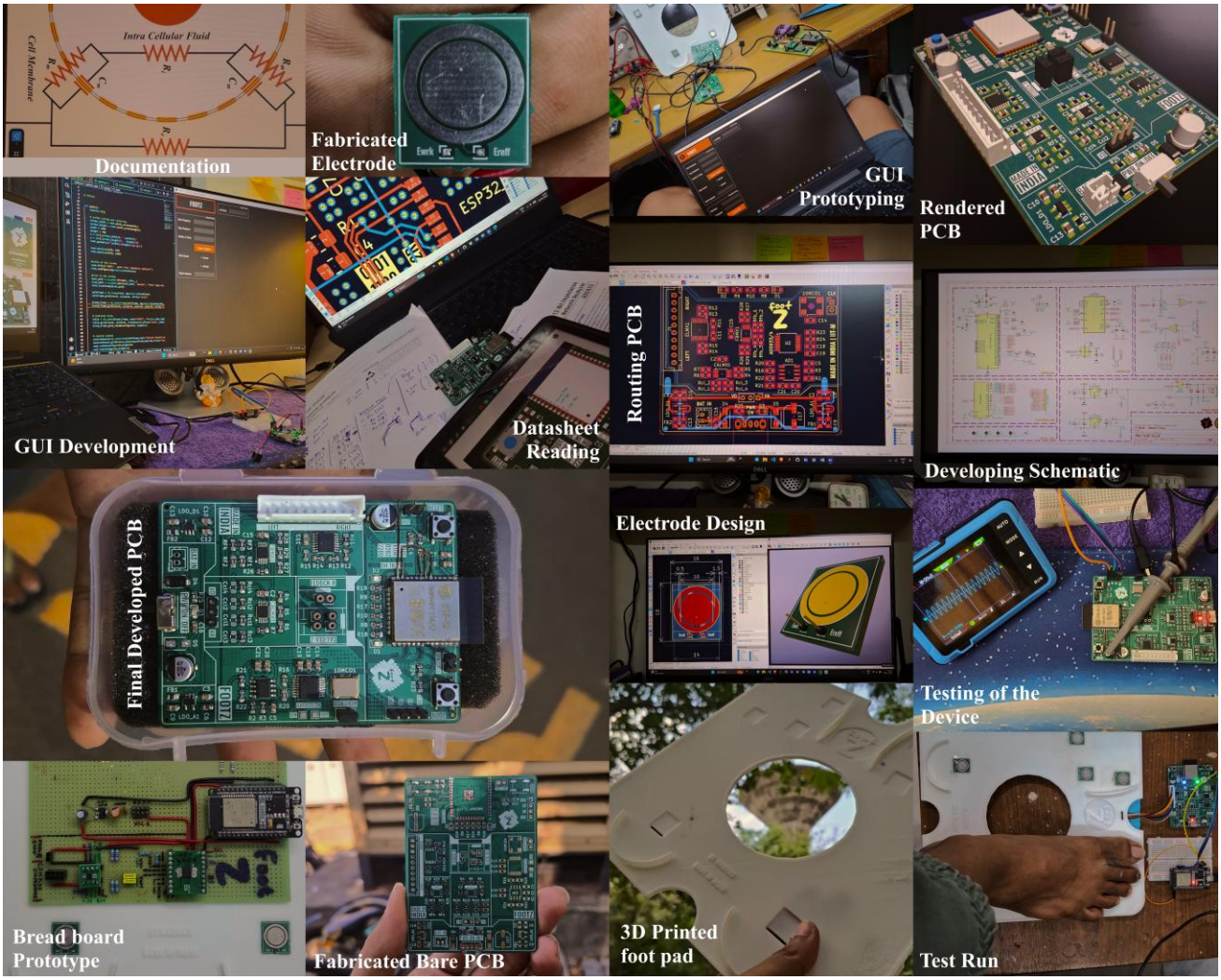

Figure 24:- Development workflow of the proposed foot bio impedance measurement system, showing the progression from theoretical modeling and electrode fabrication to schematic design, PCB development, GUI implementation, prototyping, testing, and final integrated

Chapter 6: Future Scope

- Development of a ***compact portable bioimpedance measurement device*** by integrating the existing ESP32-based PCB with a battery-powered supply system and protective enclosure.
- Implementation of a ***Python-based graphical user interface (GUI)*** for wireless control and monitoring of the device over WiFi using ESP32 Access Point (AP) mode communication.
- Development of software functionalities for real-time impedance visualization, sweep configuration, settling time adjustment, calibration control, and experimental data logging.
- Improvement of the ***signal processing and impedance extraction algorithms*** to enhance measurement stability, accuracy, and repeatability across different impedance ranges.
- Development and implementation of ***advanced multi-point calibration techniques*** across the frequency sweep to compensate for frontend parasitic effects and improve impedance estimation accuracy.
- Implementation of ***automatic ranging and feedback resistance switching mechanisms*** to avoid ADC saturation and improve acquisition of both low- and high-impedance measurements.
- Expansion of the system from magnitude-only measurements toward ***complex impedance analysis including phase*** acquisition and processing.
- Addition of external DUT testing capability for ***characterization of external RC networks*** and validation of the impedance measurement frontend.
- Future investigation of possible ***relationships between foot bioimpedance characteristics and diabetic conditions*** through larger-scale experimental data collection and pattern analysis.
- Exploration of the system as a preliminary screening and research platform for studying impedance-based changes in foot tissue properties.

Chapter 7: Reference and Data Sheet

1. G. Chand, A. K. Mishra, S. Kumar, and A. Agarwal, “Diabetic foot,” *Clinical Queries: Nephrology*, vol. 1, no. 2, pp. 144–150, 2012.
2. C. Tronstad *et al*., “Diabetic Foot Assessment using Skin Impedance in a Custom-Made Bioimpedance Spectroscopy Device,” *Sensors*, vol. 23, no. 2, 2023.
3. S. Grimnes and Ø. G. Martinsen, *Bioimpedance and Bioelectricity Basics*, 3rd ed. London, U.K.: Academic Press, 2015.
4. K. S. Cole and R. H. Cole, “Dispersion and absorption in dielectrics I. Alternating current characteristics,” *The Journal of Chemical Physics*, vol. 9, no. 4, pp. 341–351, 1941.
5. S. Gabriel, R. W. Lau, and C. Gabriel, “The dielectric properties of biological tissues: III. Parametric models for the dielectric spectrum of tissues,” *Physics in Medicine & Biology*, vol. 41, no. 11, pp. 2271–2293, 1996.
6. Analog Devices, “AD5934: High Precision Impedance Converter System Solution Datasheet,” Analog Devices Inc., Wilmington, MA, USA, 2024.
7. Analog Devices, “AN-1252: How to Configure the AD5933/AD5934,” Analog Devices Application Note, Wilmington, MA, USA, 2014.
8. H. Seoane, J. Ferreira, and J. Carmo, “A Portable Electrical Bioimpedance Measurement System Based on the AD5933 Front-End,” *IEEE Instrumentation and Measurement Magazine*, vol. 16, no. 2, pp. 42–49, Apr. 2013.
9. R. Kusche, P. Klimach, and M. Ryschka, “A Multichannel Real-Time Bioimpedance Measurement Device for Pulse Wave Analysis,” *IEEE Access*, vol. 7, pp. 57470–57480, 2019.
10. Espressif Systems, “ESP32-WROOM-32 Datasheet,” Espressif Systems, Shanghai, China, 2024.

APPENDIX A

Python Script for calibration and plotting

The main code contains GUI components which has been removed to reduce the number of pages. Only the main logic is given

```
# ======================================================
# ============ FOOTZ CORE ACQUISITION CODE ============
# ======================================================

import socket
import numpy as np

# ======================================================
# ================= WIFI SETTINGS ======================
# ======================================================

ESP32_IP = "192.168.4.1"
PORT = 5000

# ======================================================
# ================= SOCKET CONNECT =====================
# ======================================================

sock = socket.socket(socket.AF_INET, socket.SOCK_STREAM)

sock.connect((ESP32_IP, PORT))

print("Connected to FOOTZ")

# ======================================================
# ================= RECEIVE SWEEP ======================
# ======================================================

def receive_sweep():

    freqs = []

    reals = []

    imags = []

    buffer = ""

    while True:

        chunk = sock.recv(1024).decode(errors='ignore')

        if not chunk:
            continue

        buffer += chunk

        while "\n" in buffer:

            line, buffer = buffer.split("\n", 1)

            line = line.strip()
```

```
            print(line)

            # Ignore metadata
            if (
                line.startswith("START") or
                line.startswith("MODE") or
                line.startswith("CHANNEL") or
                line.startswith("RFB") or
                line.startswith("DATA")
            ):
                continue

            # Sweep complete
            if "DONE" in line:

                min_len = min(
                    len(freqs),
                    len(reals),
                    len(imags)
                )

                return (
                    np.array(freqs[:min_len]),
                    np.array(reals[:min_len]),
                    np.array(imags[:min_len])
                )

            # Parse data
            if "," in line:

                try:

                    f, r, i = line.split(",")

                    freqs.append(float(f))

                    reals.append(float(r))

                    imags.append(float(i))

                except:
                    pass

# ====================================================
# ================ CALIBRATION =======================
# ====================================================

START_FREQ = 1000
STEP_FREQ = 1000
NUM_POINTS = 100

R_CAL = 1000

print("\nRunning Calibration...\n")

cal_cmd = f"{START_FREQ},{STEP_FREQ},{NUM_POINTS},C,0,0\n"

sock.send(cal_cmd.encode())

freq_cal, real_cal, imag_cal = receive_sweep()

# Magnitude
```

```
mag_cal = np.sqrt(real_cal**2 + imag_cal**2)

# Gain Factor
G = 1 / (R_CAL * mag_cal)

# Average Gain
G_avg = np.mean(G)

print("\nCalibration Complete")
print("Gain Factor:", G_avg)

# ====================================================
# =============== FOOT MULTIPOINT SWEEP ==============
# ====================================================

foot_map = {

    0: "Right Heel",
    1: "Right Toe Pulp",
    2: "Right Toe Base",
    3: "Right Thumb",
    4: "Left Thumb",
    5: "Left Toe Base",
    6: "Left Toe Pulp",
    7: "Left Heel"
}

datasets = []

labels = []

print("\nStarting Full Foot Scan...\n")

for electrode in range(8):

    label = foot_map[electrode]

    print(f"\nScanning: {label}\n")

    # ============================================
    # Send Sweep Command
    # ============================================

    cmd = f"{START_FREQ},{STEP_FREQ},{NUM_POINTS},E,{electrode},0\n"

    sock.send(cmd.encode())

    # ============================================
    # Receive Sweep Data
    # ============================================

    freq, real, imag = receive_sweep()

    # ============================================
    # Impedance Magnitude
    # ============================================

    mag = np.sqrt(real**2 + imag**2)

    # ============================================
    # Calculate Impedance
    # ============================================
```

```
    Z = 1 / (G_avg * mag)

    datasets.append((freq, Z))

    labels.append(label)

    print(f"Completed: {label}")

# ======================================================
# ==================== PLOTTING ========================
# ======================================================

import matplotlib.pyplot as plt

fig, (ax1, ax2) = plt.subplots(2, 1, figsize=(10, 8))

# ======================================================
# ================ LINEAR PLOT =========================
# ======================================================

for i, (freq, Z) in enumerate(datasets):

    ax1.plot(
        freq,
        Z,
        linewidth=2,
        label=labels[i]
    )

ax1.set_title("Impedance vs Frequency (Linear)")

ax1.set_xlabel("Frequency (Hz)")

ax1.set_ylabel("Impedance (Ohms)")

ax1.grid(True)

ax1.legend()

# ======================================================
# ================== LOG PLOT ==========================
# ======================================================

for i, (freq, Z) in enumerate(datasets):

    ax2.plot(
        freq,
        Z,
        linewidth=2,
        label=labels[i]
    )

ax2.set_title("Impedance vs Frequency (Log Scale)")

ax2.set_xlabel("Frequency (Hz)")

ax2.set_ylabel("Impedance (Ohms)")

ax2.set_xscale("log")

ax2.set_yscale("log")
```

```
ax2.grid(True, which='both')

ax2.legend()

plt.tight_layout()

plt.show()

# ======================================================
# ==================== CLEANUP =========================
# ======================================================

sock.close()

print("\nFOOTZ Scan Complete\n")
```

APPENDIX B

Arduino Script for AD5934 I2C control and UART data transfer

```
#include <WiFi.h>
#include <Wire.h>

#define AD5934_ADDR 0x0D

// ================ LEDs ================
#define GREEN_LED 25
#define BLUE_LED  26

// ================ BUZZER ================
#define BUZZER_PIN 14

// ================ CAL MUX ================
#define CALMUX_EN 23
#define CALMUX_A0 16
#define CALMUX_A1 17

// ================ ELECTRODE MUX ================
#define ELECMUX_EN 19
#define ELECMUX_A0 16
#define ELECMUX_A1 17
#define ELECMUX_A2 18

// ================ RFB MUX ================
#define RFBMUX_EN 27
#define RFBMUX_A0 32
#define RFBMUX_A1 33

// ================ WIFI ================
const char* ssid = "FOOTZ-IITM";
const char* password = "12345678";

WiFiServer server(5000);
WiFiClient client;

// ================ AD5934 ================
#define MCLK 10000000.0

// ======================================================
// ====================== TONES =========================
// ======================================================

void toneSimple(int freq, int duration) {

  ledcAttachPin(BUZZER_PIN, 0);

  ledcSetup(0, freq, 8);

  ledcWrite(0, 128);

  delay(duration);

  ledcWrite(0, 0);
```

```
  delay(20);
}

// ======================================================
// ==================== BOOT TONE =======================
// ======================================================

void bootTone() {

  int notes[] = {
    900,
    1100,
    1400,
    1700,
    2100
  };

  int durations[] = {
    120,
    120,
    140,
    160,
    240
  };

  for (int i = 0; i < 5; i++) {

    digitalWrite(GREEN_LED, HIGH);
    digitalWrite(BLUE_LED, LOW);

    toneSimple(notes[i], durations[i]);

    digitalWrite(GREEN_LED, LOW);
    digitalWrite(BLUE_LED, HIGH);

    delay(40);
  }

  digitalWrite(BLUE_LED, LOW);
}

// ======================================================
// ================= CONNECT TONE =======================
// ======================================================

void connectTone() {

  int notes[] = {
    1200,
    1500,
    1800,
    2100,
    2400
  };

  int durations[] = {
    70,
    70,
    70,
    90,
    180
```

```
  };

  for (int i = 0; i < 5; i++) {

    toneSimple(notes[i], durations[i]);

    delay(25);
  }

  digitalWrite(GREEN_LED, HIGH);
}

// ======================================================
// ================= DISCONNECT TONE ====================
// ======================================================

void disconnectTone() {

  int notes[] = {
    1200,
    900,
    700
  };

  int durations[] = {
    100,
    120,
    200
  };

  for (int i = 0; i < 3; i++) {

    toneSimple(notes[i], durations[i]);

    delay(20);
  }

  digitalWrite(GREEN_LED, LOW);
}

// ======================================================
// ================= SWEEP START TONE ===================
// ======================================================

void sweepStartTone() {

  toneSimple(1600, 180);

  delay(70);

  toneSimple(2100, 220);
}

// ======================================================
// ================== SWEEP END TONE ====================
// ======================================================

void sweepEndTone() {

  toneSimple(1100, 320);
}
```

```
// ====================================================
// ================= LOW LEVEL I2C ====================
// ====================================================

void writeReg(uint8_t reg, uint8_t val) {

  Wire.beginTransmission(AD5934_ADDR);

  Wire.write(reg);

  Wire.write(val);

  Wire.endTransmission();
}

uint8_t readReg(uint8_t reg) {

  Wire.beginTransmission(AD5934_ADDR);

  Wire.write(reg);

  Wire.endTransmission(false);

  Wire.requestFrom(AD5934_ADDR, 1);

  if (Wire.available())
    return Wire.read();

  return 0;
}

void setControl(uint16_t cmd) {

  writeReg(0x80, (cmd >> 8) & 0xFF);

  writeReg(0x81, cmd & 0xFF);
}

// ====================================================
// ================= FREQUENCY CONFIG =================
// ====================================================

uint32_t freqToReg(float freq) {

  return (uint32_t)((freq * (1ULL << 27) * 16) / MCLK);
}

void setStartFreq(float freq) {

  uint32_t code = freqToReg(freq);

  writeReg(0x82, code >> 16);

  writeReg(0x83, code >> 8);

  writeReg(0x84, code);
}

void setIncrement(float freq) {

  uint32_t code = freqToReg(freq);
```

```
  writeReg(0x85, code >> 16);

  writeReg(0x86, code >> 8);

  writeReg(0x87, code);
}

void setNumIncrements(int n) {

  writeReg(0x88, n >> 8);

  writeReg(0x89, n);
}

// ======================================================
// ==================== DATA READ =======================
// ======================================================

int16_t readReal() {

  return (int16_t)((readReg(0x94) << 8) | readReg(0x95));
}

int16_t readImag() {

  return (int16_t)((readReg(0x96) << 8) | readReg(0x97));
}

uint8_t getStatus() {

  return readReg(0x8F);
}

bool waitDataReady(uint32_t timeoutMs = 1000) {

  uint32_t start = millis();

  while (!(getStatus() & 0x02)) {

    if (millis() - start > timeoutMs)
      return false;

    delay(1);
  }

  return true;
}

// ======================================================
// ================= AD5934 CONFIG ======================
// ======================================================

void configureAD5934(float startFreq,
                     float stepFreq,
                     int numPoints) {

  setControl(0x8000);

  delay(10);

  setControl(0xB000);
```

```
  writeReg(0x80, 0x01);

  writeReg(0x81, 0x00);

  setStartFreq(startFreq);

  setIncrement(stepFreq);

  setNumIncrements(numPoints);

  writeReg(0x8A, 0x00);

  writeReg(0x8B, 0x20);
}

// ====================================================
// ==================== MUX CONTROL ===================
// ====================================================

void disableAllMux() {

  digitalWrite(CALMUX_EN, LOW);

  digitalWrite(ELECMUX_EN, LOW);
}

void selectCalMux(uint8_t ch) {

  digitalWrite(ELECMUX_EN, LOW);

  digitalWrite(CALMUX_EN, HIGH);

  digitalWrite(CALMUX_A0, ch & 0x01);

  digitalWrite(CALMUX_A1, (ch >> 1) & 0x01);
}

void selectElecMux(uint8_t ch) {

  digitalWrite(CALMUX_EN, LOW);

  digitalWrite(ELECMUX_EN, HIGH);

  digitalWrite(ELECMUX_A0, ch & 0x01);

  digitalWrite(ELECMUX_A1, (ch >> 1) & 0x01);

  digitalWrite(ELECMUX_A2, (ch >> 2) & 0x01);
}

void selectRfb(uint8_t rfb_sel) {

  digitalWrite(RFBMUX_EN, HIGH);

  digitalWrite(RFBMUX_A0, rfb_sel & 0x01);

  digitalWrite(RFBMUX_A1, (rfb_sel >> 1) & 0x01);
}

// ====================================================
// ==================== RUN SWEEP =====================
// ====================================================
```

```
void runSweep(float startFreq,
              float stepFreq,
              int numPoints,
              char mode,
              int channel,
              int rfb) {

  // -------- LED + Tone --------
  digitalWrite(BLUE_LED, HIGH);

  sweepStartTone();

  // -------- MUX Selection --------
  selectRfb(rfb);

  if (mode == 'E')
    selectElecMux(channel);

  else if (mode == 'C')
    selectCalMux(channel);

  delay(20);

  // -------- Configure --------
  configureAD5934(startFreq, stepFreq, numPoints);

  // -------- Init Sweep --------
  setControl(0x1000);

  delay(50);

  setControl(0x2000);

  // -------- Send Metadata --------
  client.println("START");

  client.print("MODE:");
  client.println(mode);

  client.print("CHANNEL:");
  client.println(channel);

  client.print("RFB:");
  client.println(rfb);

  client.println("DATA");

  // -------- Sweep --------
  float freq = startFreq;

  for (int i = 0; i < numPoints; i++) {

    if (!waitDataReady()) {

      client.println("ERROR:TIMEOUT");

      break;
    }

    int16_t real = readReal();
```

```
      int16_t imag = readImag();

      client.print(freq, 2);

      client.print(",");

      client.print(real);

      client.print(",");

      client.println(imag);

      if (getStatus() & 0x04)
        break;

      setControl(0x3000);

      freq += stepFreq;
    }

    client.println("DONE");

    digitalWrite(BLUE_LED, LOW);

    sweepEndTone();
}

// ======================================================
// ==================== WIFI SETUP ======================
// ======================================================

void setupWiFi() {

    WiFi.mode(WIFI_AP);

    WiFi.softAP(ssid, password);

    IPAddress IP = WiFi.softAPIP();

    Serial.println();

    Serial.println("================================");

    Serial.println("FOOTZ-IITM AP STARTED");

    Serial.print("IP Address: ");

    Serial.println(IP);

    Serial.println("Port: 5000");

    Serial.println("================================");

    server.begin();
}

// ======================================================
// ====================== SETUP =========================
// ======================================================

void setup() {
```

```
  Serial.begin(115200);

  Wire.begin();

  // -------- LED --------
  pinMode(GREEN_LED, OUTPUT);

  pinMode(BLUE_LED, OUTPUT);

  // -------- BUZZER --------
  pinMode(BUZZER_PIN, OUTPUT);

  // -------- CAL MUX --------
  pinMode(CALMUX_EN, OUTPUT);

  pinMode(CALMUX_A0, OUTPUT);

  pinMode(CALMUX_A1, OUTPUT);

  // -------- ELEC MUX --------
  pinMode(ELECMUX_EN, OUTPUT);

  pinMode(ELECMUX_A0, OUTPUT);

  pinMode(ELECMUX_A1, OUTPUT);

  pinMode(ELECMUX_A2, OUTPUT);

  // -------- RFB MUX --------
  pinMode(RFBMUX_EN, OUTPUT);

  pinMode(RFBMUX_A0, OUTPUT);

  pinMode(RFBMUX_A1, OUTPUT);

  disableAllMux();

  // -------- Boot Animation --------
  for (int i = 0; i < 3; i++) {

    digitalWrite(GREEN_LED, HIGH);

    digitalWrite(BLUE_LED, HIGH);

    delay(150);

    digitalWrite(GREEN_LED, LOW);

    digitalWrite(BLUE_LED, LOW);

    delay(150);
  }

  bootTone();

  // -------- WiFi --------
  setupWiFi();
}

// ====================================================
// ======================== LOOP ======================
// ====================================================
```

```
void loop() {

  // ========================================
  // Wait for client
  // ========================================

  if (!client || !client.connected()) {

    WiFiClient newClient = server.available();

    if (newClient) {

      client = newClient;

      digitalWrite(GREEN_LED, HIGH);

      connectTone();

      Serial.println("Client Connected");
    }
  }

  // ========================================
  // Handle disconnect
  // ========================================

  if (client && !client.connected()) {

    client.stop();

    digitalWrite(GREEN_LED, LOW);

    disconnectTone();

    Serial.println("Client Disconnected");
  }

  // ========================================
  // Receive command
  // ========================================

  if (client &&
      client.connected() &&
      client.available()) {

    String cmd = client.readStringUntil('\n');

    cmd.trim();

    Serial.print("CMD: ");

    Serial.println(cmd);

    // ====================================
    // Expected:
    // start,step,points,mode,ch,rfb
    // Example:
    // 1000,1000,100,E,3,1
    // ====================================

    float startFreq = 0;
```

```
      float stepFreq = 0;

      int points = 0;

      char mode = 'E';

      int channel = 0;

      int rfb = 0;

      int idx1 = cmd.indexOf(',');

      int idx2 = cmd.indexOf(',', idx1 + 1);

      int idx3 = cmd.indexOf(',', idx2 + 1);

      int idx4 = cmd.indexOf(',', idx3 + 1);

      int idx5 = cmd.indexOf(',', idx4 + 1);

      if (idx1 > 0 &&
          idx2 > 0 &&
          idx3 > 0 &&
          idx4 > 0 &&
          idx5 > 0) {

        startFreq = cmd.substring(0, idx1).toFloat();

        stepFreq = cmd.substring(idx1 + 1, idx2).toFloat();

        points = cmd.substring(idx2 + 1, idx3).toInt();

        mode = cmd.substring(idx3 + 1, idx4).charAt(0);

        channel = cmd.substring(idx4 + 1, idx5).toInt();

        rfb = cmd.substring(idx5 + 1).toInt();

        runSweep(startFreq,
                 stepFreq,
                 points,
                 mode,
                 channel,
                 rfb);
      }

      else {

        client.println("ERROR:INVALID_COMMAND");
      }
    }
  }
```

APPENDIX C

Raw plots of different parts of the body

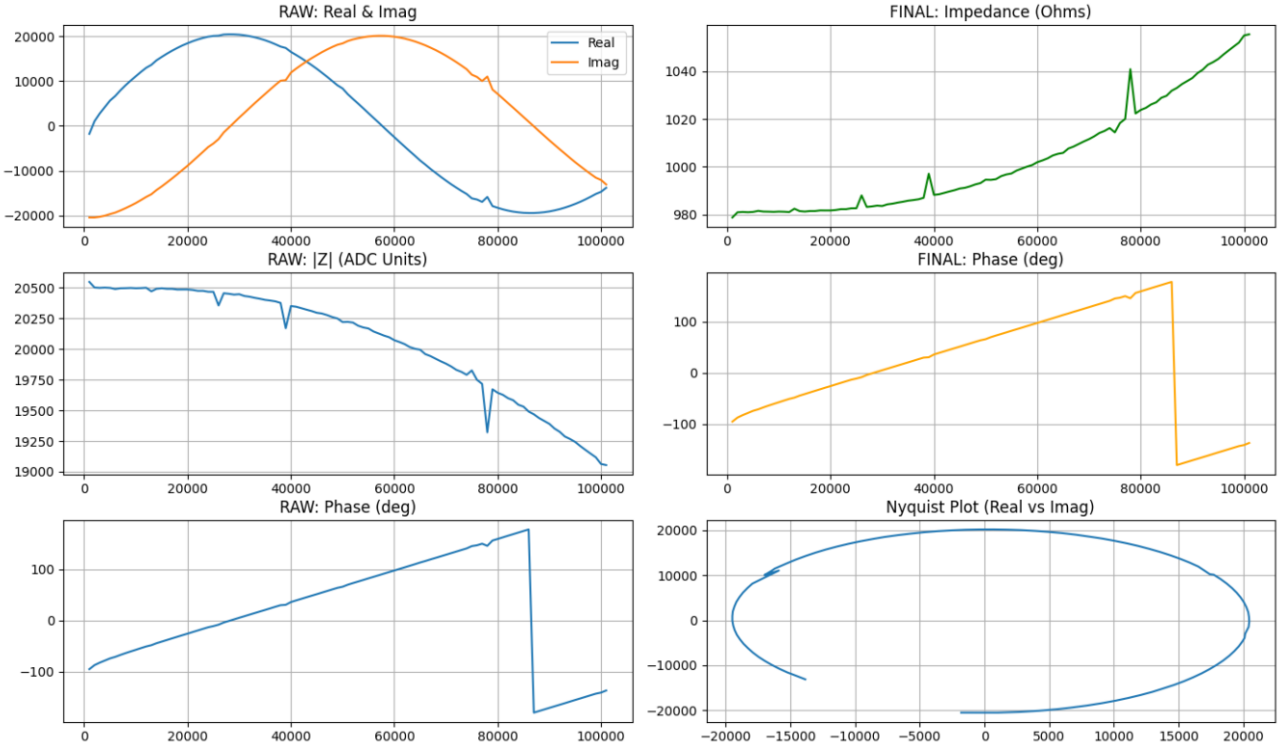

Short Circuit Test

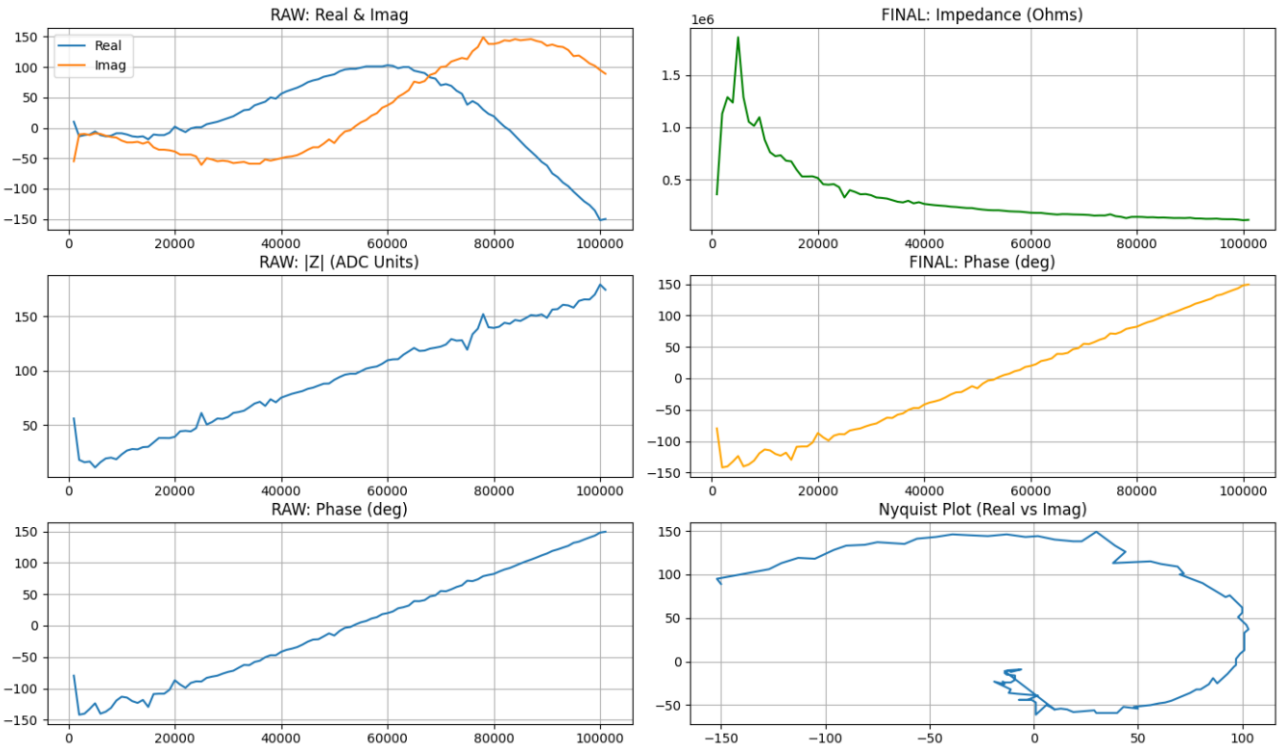

Open Circuit Test

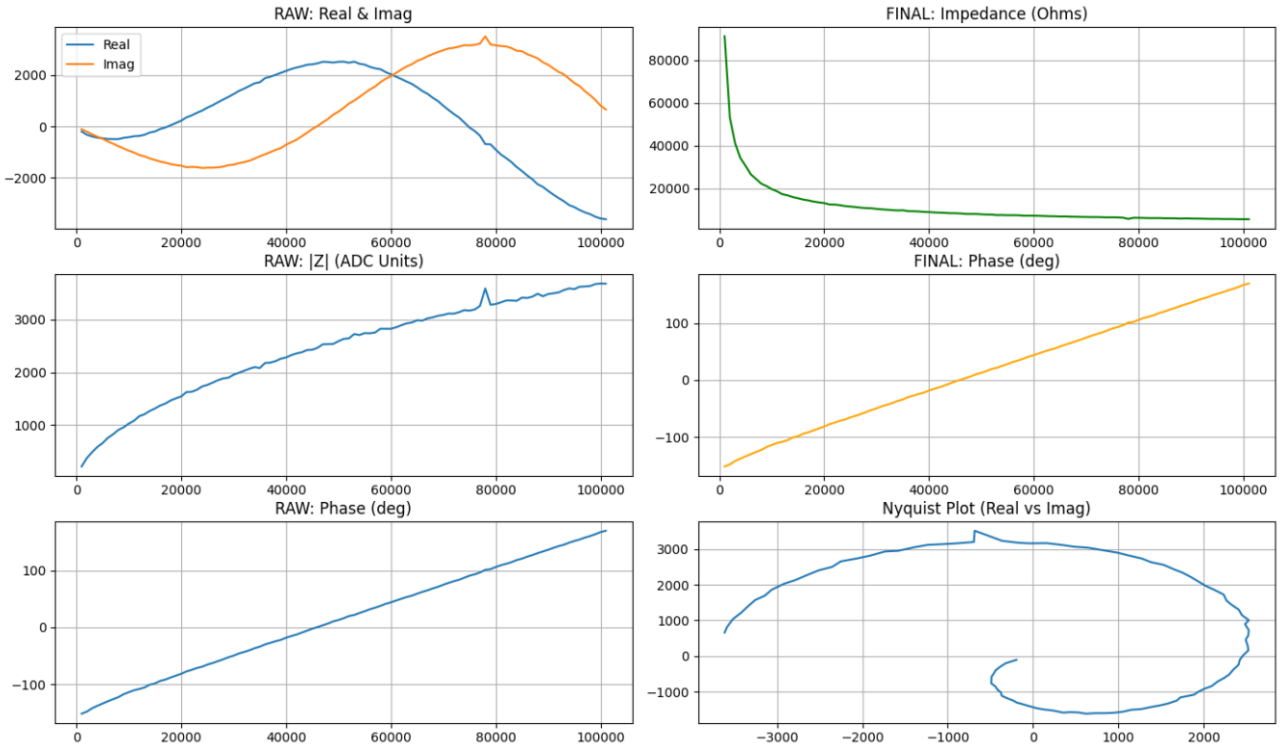

Ankle Test

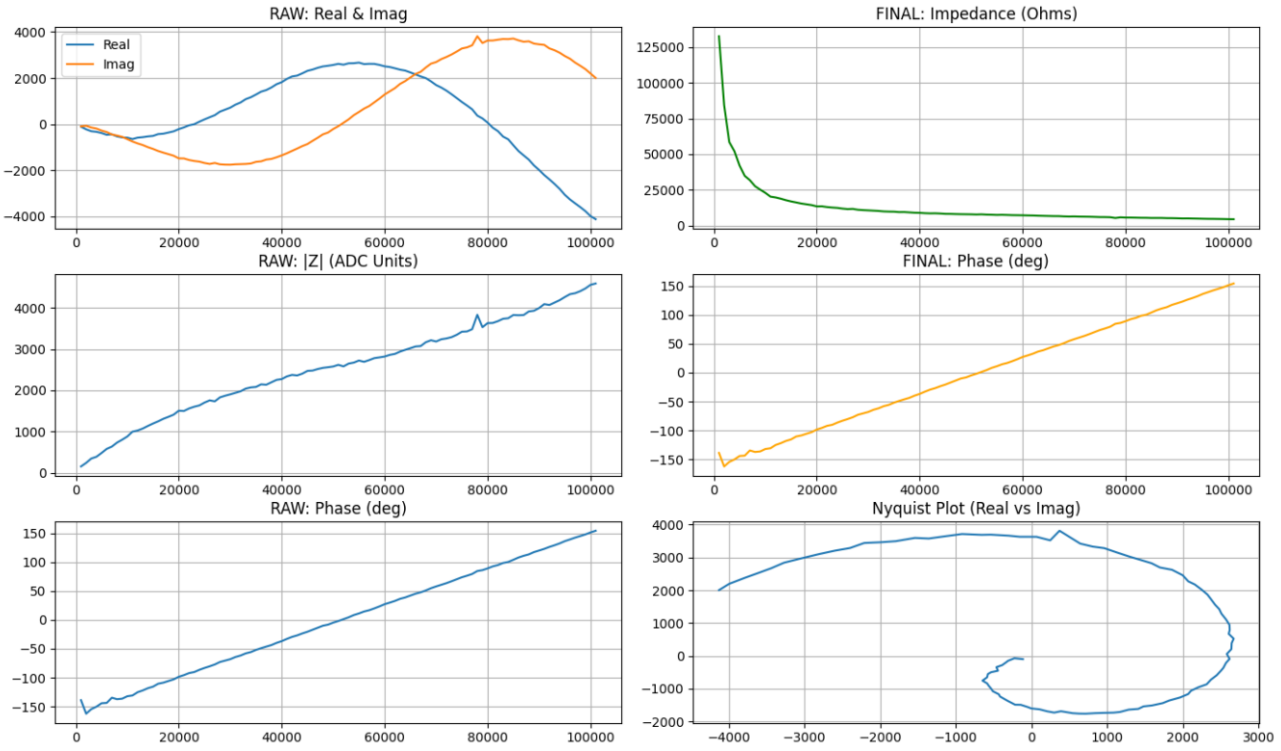

Elbow Test

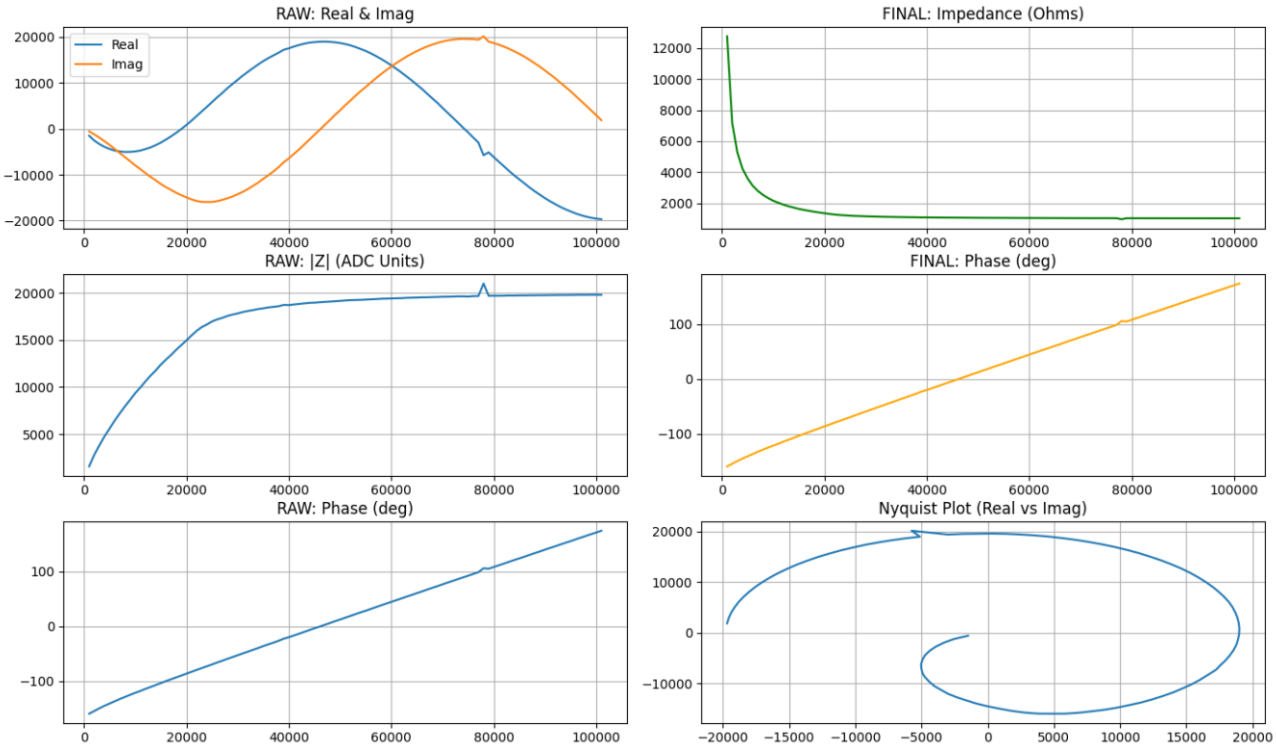

Foot Heel Test

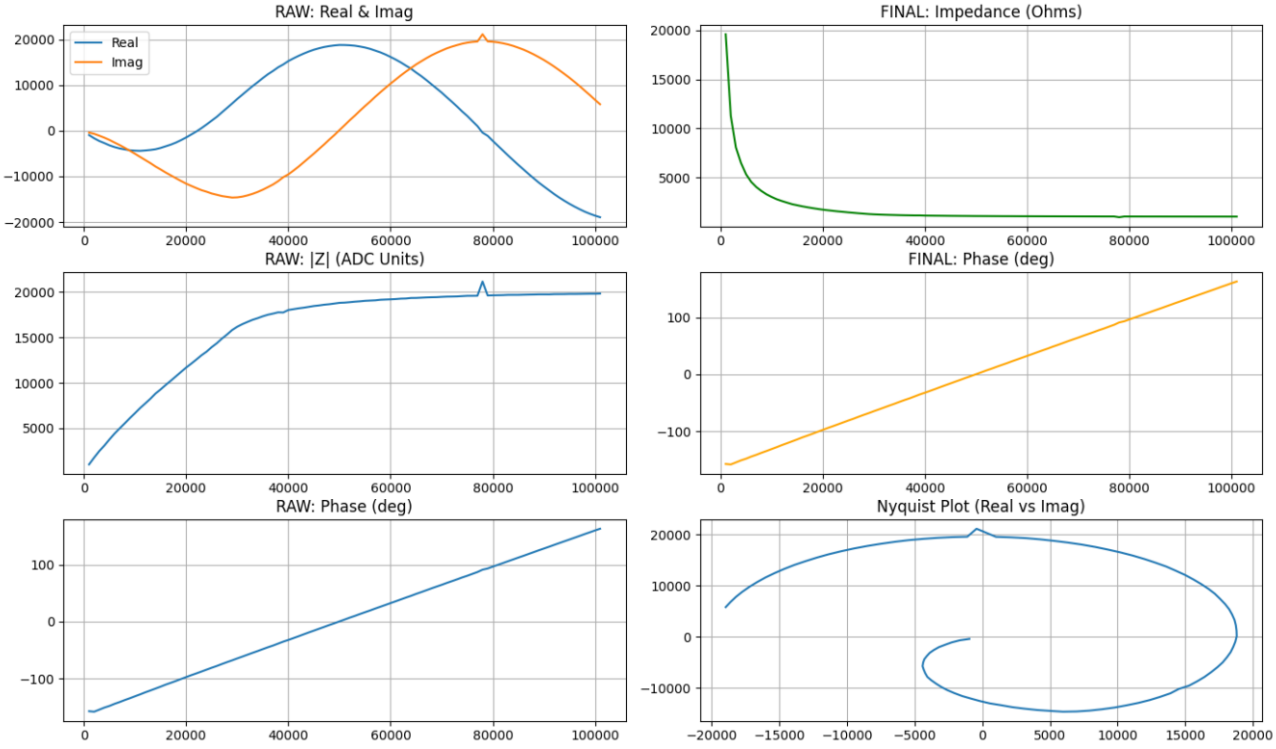

Hand Thumb Test

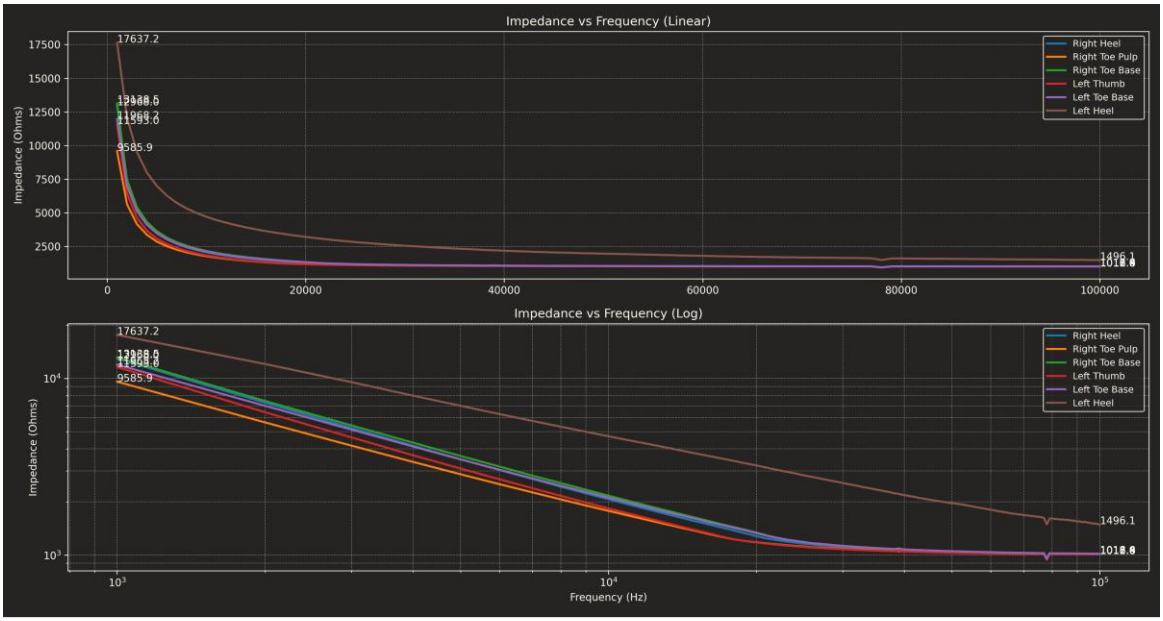
Impedance vs Frequency (Linear)
Impedance (Ohms)
17637.2
9585.9
1496.1
Impedance vs Frequency (Log)
Impedance (Ohms)
Frequency (Hz)
Right Heel
Right Toe Pulp
Right Toe Base
Left Thumb
Left Toe Base
Left Heel

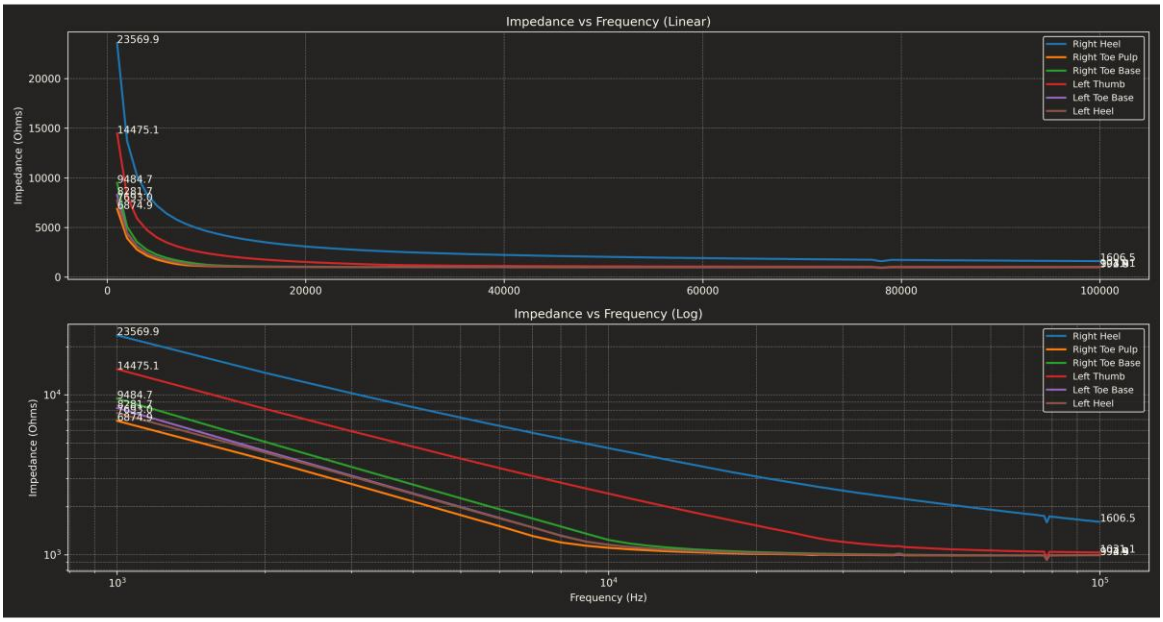
Impedance vs Frequency (Linear)
Impedance (Ohms)
23569.9
14475.1
9484.7
1606.5
Impedance vs Frequency (Log)
Impedance (Ohms)
Frequency (Hz)
Right Heel
Right Toe Pulp
Right Toe Base
Left Thumb
Left Toe Base
Left Heel

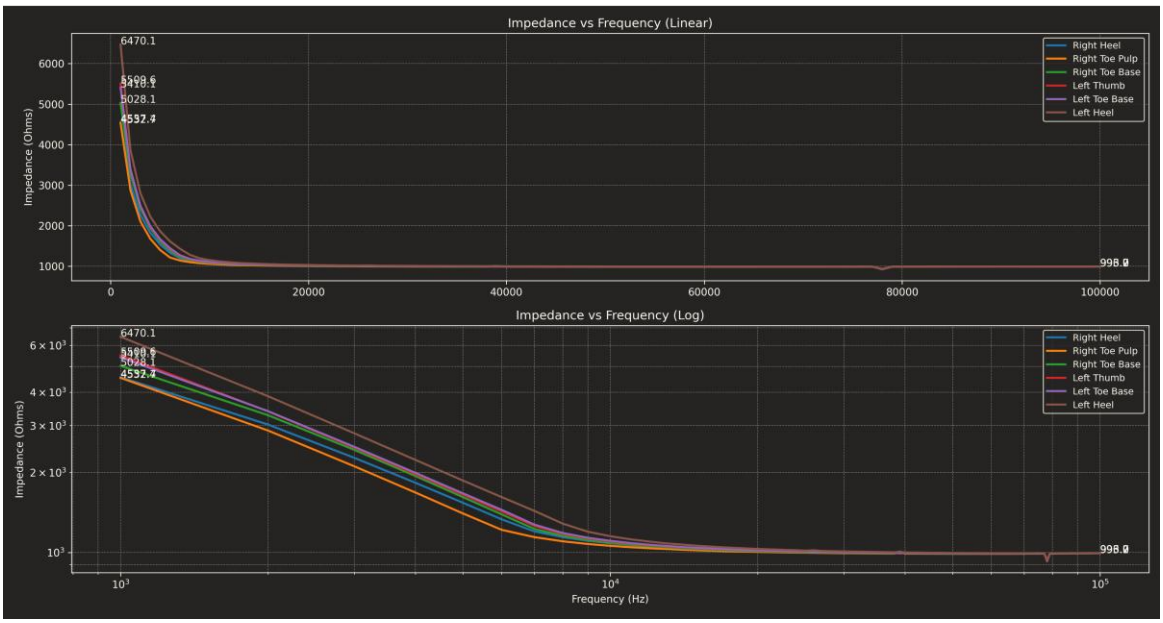
Impedance vs Frequency (Linear)
Impedance (Ohms)
6470.1
5028.1
Impedance vs Frequency (Log)
Impedance (Ohms)
Frequency (Hz)
Right Heel
Right Toe Pulp
Right Toe Base
Left Thumb
Left Toe Base
Left Heel

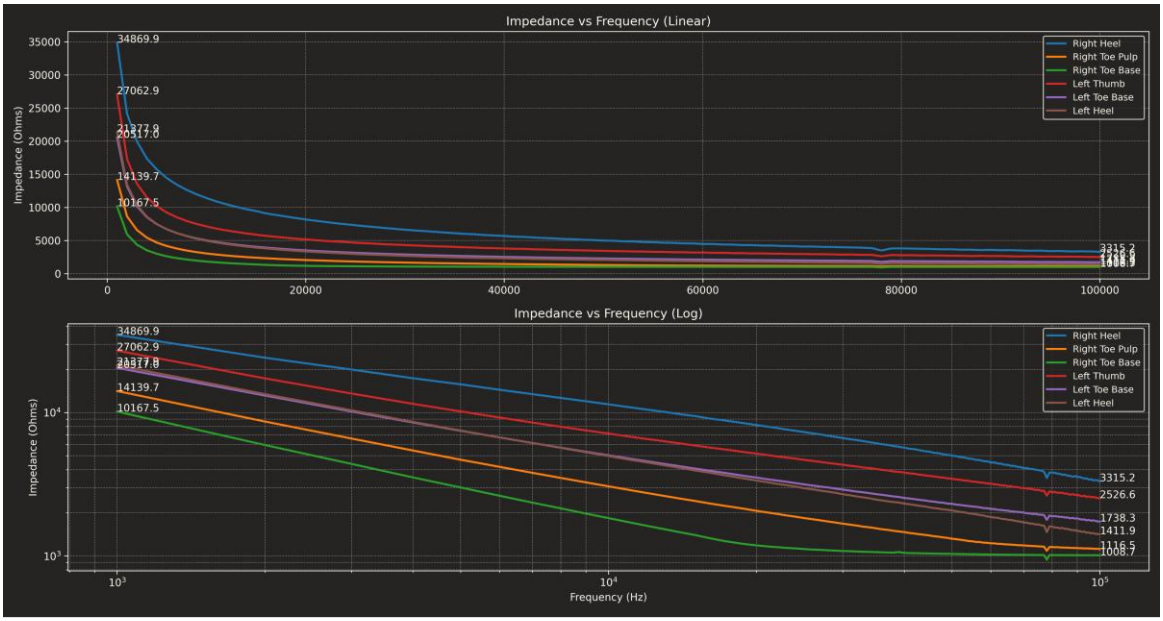
Impedance vs Frequency (Linear)
Impedance (Ohms)
Right Heel
Right Toe Pulp
Right Toe Base
Left Thumb
Left Toe Base
Left Heel
34869.9
27062.9
14139.7
10167.5
Impedance vs Frequency (Log)
3315.2
2526.6
1738.3
1411.9
1116.5
1008.7
Frequency (Hz)

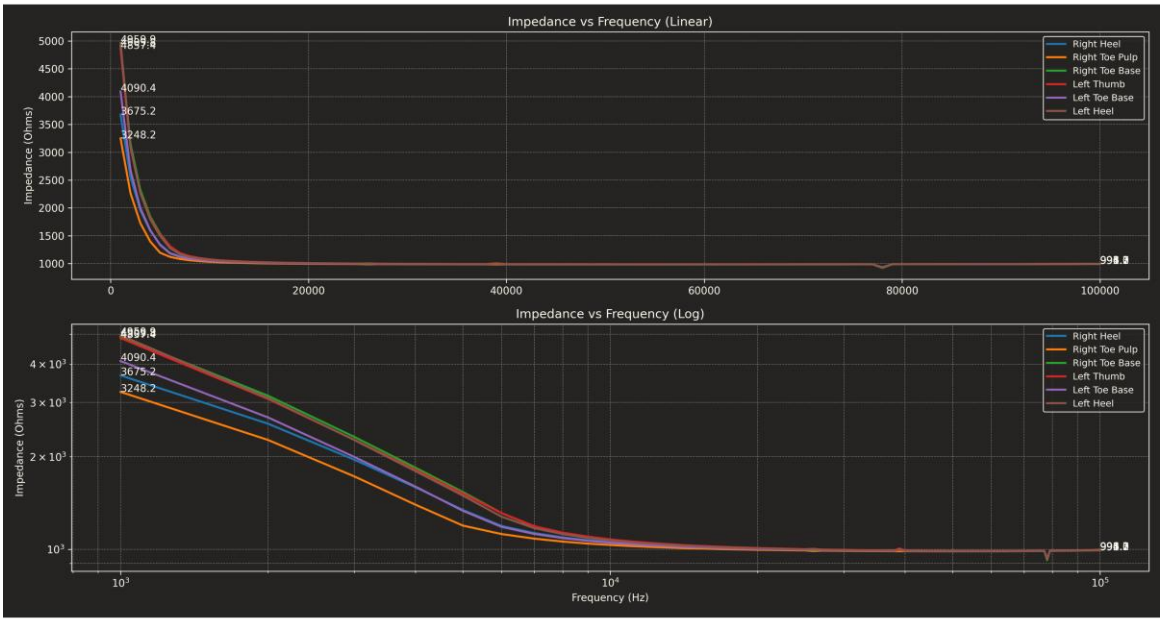
Impedance vs Frequency (Linear)
Impedance (Ohms)
Right Heel
Right Toe Pulp
Right Toe Base
Left Thumb
Left Toe Base
Left Heel
4090.4
3675.2
3248.2
Impedance vs Frequency (Log)
Frequency (Hz)

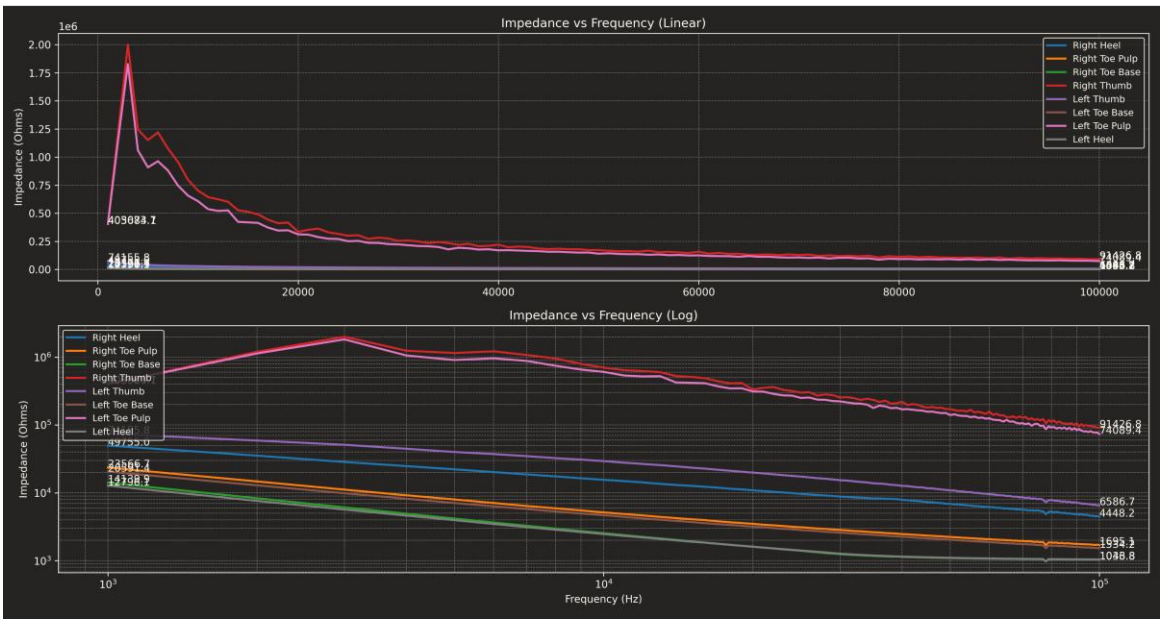
Impedance vs Frequency (Linear)
Impedance (Ohms)
Right Heel
Right Toe Pulp
Right Toe Base
Right Thumb
Left Thumb
Left Toe Base
Left Toe Pulp
Left Heel
Impedance vs Frequency (Log)
91426.8
74099.4
6586.7
4448.2
Frequency (Hz)